

# Deep Learning on Monocular Object Pose Detection and Tracking: A Comprehensive Overview

Zhaixin Fan\*, Yazhi Zhu<sup>†</sup>, Yulin He\*, Qi Sun\*, Hongyan Liu<sup>†</sup>, and Jun He\*

\*Renmin University of China    <sup>†</sup>Tsinghua University    <sup>‡</sup>Beijing Jiaotong University

**Abstract**—Object pose detection and tracking has recently attracted increasing attention due to its wide applications in many areas, such as autonomous driving, robotics, and augmented reality. Among methods for object pose detection and tracking, deep learning is the most promising one that has shown better performance than others. However, there is lack of survey study about latest development of deep learning based methods. Therefore, this paper presents a comprehensive review of recent progress in object pose detection and tracking that belongs to the deep learning technical route. To achieve a more thorough introduction, the scope of this paper is limited to methods taking monocular RGB/RGBD data as input, covering three kinds of major tasks: instance-level monocular object pose detection, category-level monocular object pose detection, and monocular object pose tracking. In our work, metrics, datasets, and methods about both detection and tracking are presented in detail. Comparative results of current state-of-the-art methods on several publicly available datasets are also presented, together with insightful observations and inspiring future research directions.

**Index Terms**—Object Pose Detection, Object Pose Tracking, Instance Level, Category Level, Monocular.

## 1 INTRODUCTION

Object pose detection and tracking is a critical problem in the computer vision field and have been extensively studied in the past decades. It is closely related to many rapidly evolving technological areas such as autonomous driving, robotics, and augmented reality.

For autonomous driving [1]–[4], the task is often called 3D object detection (tracking). It can provide self-driving cars with accurate positional and orientational information of other objects on the road, thus helping the cars avoid possible collisions or accidents in advance. For robotics [5]–[8], the estimated object pose can provide the robot with positional information for grasping, navigation, and other actions related to environmental interaction. For augmented reality [9]–[12], the estimated object pose can provide sufficient information for 2D-3D interaction. For example, projection from real-world to image can be achieved using the estimated object pose so that further actions such as special effects injection can be done.

Traditional methods [13]–[16] use handcrafted features and optimization algorithms to detect or track object pose. These methods have been researched for a long time and have attracted exhaustive attention. However, with deep learning becoming popular, studies about this kind of methods become less, and deep learning methods are proliferating. Previous surveys [17]–[19] have provided comprehensive review for this kind of methods. But there is no survey focusing on *deep learning on object pose detection and tracking*. A comprehensive review of recent progress in this field is more difficult and challenging, as many works have been proposed and the quantity is constantly updated every year.

*Corresponding author: J. He.*

This paper aims to provide an in-depth survey of current state-of-the-art deep learning methods for object pose detection and tracking. To avoid being overbroad and provide a more detailed analysis, we only study deep learning-based monocular object pose detection and tracking. Note, “Monocular” in this paper refers to the situation that input data of model is RGB or RGBD images captured by a single monocular camera. Therefore, this survey does not involve methods taking point cloud captured by LiDAR or RGBD images captured by stereo cameras as input.

In Table 1, we show what tasks we consider in this survey. Specifically, this survey cares about two major tasks: monocular object pose detection and monocular object pose tracking. We will introduce them both from the perspective of instance-level and category-level. Hence, these two major tasks can be divided into four subtasks: instance-level object pose detection, category-level object pose detection, instance-level object pose tracking, and category-level object pose tracking. However, for tracking tasks, as the field is in a relatively immature development stage, there is only a small number of related works. Besides, outputs of the two tasks are unified. Therefore, we combine the two tasks as a unified task in our survey. Note, unless otherwise specified, “objects” in this survey refers to rigid objects.

In the progress of our research, we find there have already some survey works about Object Pose Detection [17]–[22]. The differences between these works and this paper include following aspects. 1) Previous works involve both traditional methods and deep learning methods, while we mainly focus on researching and analyzing state-of-the-art deep learning models in a very detailed manner. 2) Previous works review methods taking all kinds of input data formats as input in a coarse manner, while we only

Tasks	Subtasks	Input	Output
Monocular object pose detection	Instance level object pose detection	RGB/RGBD image+CAD	Rotation and translation
	Category level object pose detection	RGB/RGBD image	Rotation, translation and object size
Monocular object pose tracking	Instance level object pose tracking	RGB/RGBD video+initial pose+CAD	Rotation and translation
	Category level object pose tracking	RGB/RGBD video+initial pose	Rotation and translation

TABLE 1  
Tasks we consider in this survey.

introduce monocular methods in a fine-grained way. 3) Some of the previous works don't introduce task definition and metrics definition, which would make the scope of their surveys obscure. In our work, we define them in detail to provide readers with a clear understanding of this field. 4) Few previous works introduce current large-scale datasets in detail. However, datasets play a crucial role in deep learning. Therefore, we present a comprehensive description and comparison of existing open-source datasets in this survey. 5) Previous works don't review works concerning object pose tracking. We argue that pose detection and pose tracking are highly related. Hence, it is necessary to analyze them in one unified work. 6) Few previous works analyze current challenges and possible future works. In this paper we give suggestions for future works and corresponding reasons after introducing existing works.

**Contribution:** The major contributions of this work can be summarized as follows:

- To the best of our knowledge, this is the first survey that comprehensively covers task definition, metrics definition, datasets, and intact detailed illustration of deep learning-based object pose detection and tracking methods with monocular RGB/RGBD input. Note that in contrast to existing reviews, we focus on deep learning methods for monocular RGB/RGBD image input rather than all types of data format.
- This paper addresses the most recent and advanced progress of object pose detection and tracking. Thus, it provides readers with an insight into the most cutting-edge technologies, which benefits both academia and industry.
- Full comparison and analysis of state-of-the-art methods are presented. They are compared both qualitatively and quantitatively. Hence, the advantages and disadvantages of different techniques are clear at a glance.
- We have provided comprehensive analysis for potential future research directions and challenges, which may be helpful for readers to find possible breakthrough points that may benefit their future works from a variety of different perspectives.

**Organization:** An overview of this survey is shown in Figure 1. In our work, as mentioned above, the monocular object pose detection and tracking task can be classified into four subtasks, among which instance-level object pose tracking and category-level object pose tracking are combined as a unified task for better literature classification and better logical organization. This means that instance level monocular object pose detection, category level monocular object pose detection and monocular object pose tracking are defined as three horizontal tasks in this survey. Therefore,

there are three kinds of tasks being organized and introduced in our work as shown in Figure 1.

Specifically, first, in Section 2, we introduce the detailed definitions of the three tasks and some most commonly used metrics for evaluating object pose detection (tracking) algorithms. After that, datasets used to train and test deep learning models are presented and compared in Section 3. Then, techniques about the three tasks are reviewed in detail in Section 4, Section 5 and Section 6 respectively with fine-grained classifications. A complete comparison of these methods is also presented both qualitatively and quantitatively. Finally, we analyze future research directions and challenges in Section 7 and conclude our work in Section 8.

## 2 TASKS AND METRICS DEFINITION

Before reviewing relevant works, we first define the three tasks discussed in this paper and introduce some commonly used metrics in this section. Illustrations of the three tasks are shown in Figure 2. An overview of their input and output can also be found in Table 1.

### 2.1 Tasks Definition

**Instance level monocular object pose detection:** Given a monocular RGB/RGBD image  $\mathcal{I}$  and a CAD model  $\mathcal{M}$  of a target instance, we need to recover the object pose  $\mathcal{P} \in SE(3)$  of the target instance observed in the image, where  $\mathcal{P}$  can be decoupled to rotation  $\mathcal{R} \in SO(3)$  and translation  $\mathcal{T} \in R^3$  w.r.t the camera. The rotation  $\mathcal{R}$  consists of pitch, yaw and roll, which refer to rotations around the X-axis, the Y-axis, and the Z-axis respectively. They constitute the object's rotation around the overall 3D space. Translation  $\mathcal{T}$  refers to the x, y, z components of the object center in the camera coordinate system.  $\mathcal{P}$  can also be understood from another perspective as a function of transforming an object from its object coordinate system to the camera coordinate system. The whole task can be expressed as:

$$[\mathcal{R}|\mathcal{T}] = \mathcal{F}\{[\mathcal{I}, \mathcal{M}|\theta]\}$$

where  $\mathcal{F}$  refers to a specific deep learning model, and  $\theta$  refers to the model's parameters. In the task, rotation and translation together form 6 degrees of freedom (6Dof). Note that a well-trained model only works for detecting a specific object instance.

**Category level monocular object pose detection:** Given a monocular RGB/RGBD image  $\mathcal{I}$ , we need to recover the pose  $\mathcal{P} \in SE(3)$  of the target object in the image with no CAD model available. Besides, object size  $\mathcal{S} \in R^3$  (i.e. object length, width and height) also needs to be estimated. In the category-level monocular object pose detection task, a well-trained model should obtain the ability to recognize a line of object instances that belong to the same category. Rotation, translation and object size together form 9 degrees

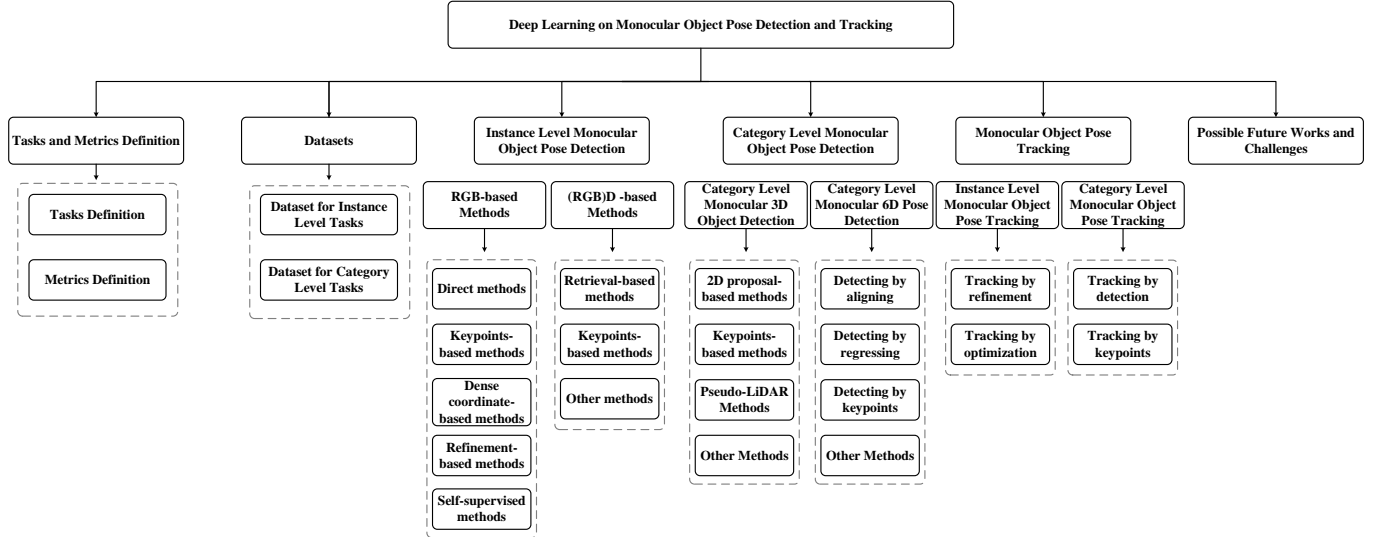


Fig. 1. A taxonomy of deep learning methods for monocular object pose detection and tracking

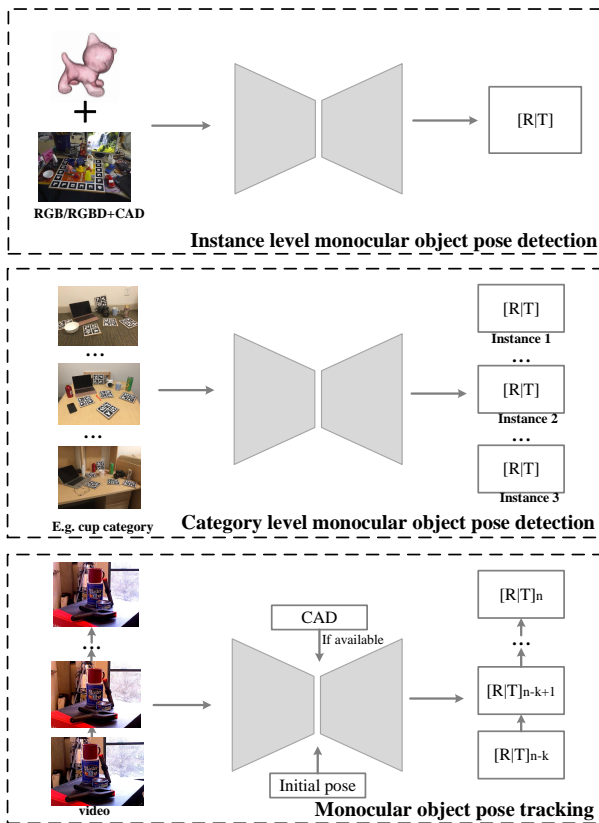


Fig. 2. Illustrations of tasks involved in this survey.

of freedom (9Dof). Thus, strictly speaking, the task should be defined as category-level monocular 9Dof pose detection. In addition, in some works, especially in an autonomous driving scenario, only the 7Dof pose is required to be predicted, where the pitch and roll are excluded. The task can be expressed as:

$$[\mathcal{R}|\mathcal{T}|\mathcal{S}] = \mathcal{F}\{[\mathcal{I}|\theta]\}$$

where  $\mathcal{F}$  refers to a specific deep learning model and  $\theta$  refers

to model parameters.

**Monocular object pose tracking:** Given a series of monocular RGB/RGBD images  $\mathcal{I}_{n-k}, \mathcal{I}_{n-k+1}, \dots, \mathcal{I}_n$  from time steps  $T_{n-k}$  to  $T_n$  and the initial 6D pose  $\mathcal{P}_0$  of the target object, we need to recover poses of the target object at all time steps. The task at time step  $T_n$  can be expressed as:

$$\mathcal{P}_n = \mathcal{F}\{\mathcal{I}_n, \dots, \mathcal{I}_{n-k+1}, \mathcal{I}_{n-k}; \mathcal{P}_0 | \theta\}$$

where  $\mathcal{F}$  refers to the tracking algorithm and  $\theta$  refers to the model's parameters. The task can also be divided into instance-level object pose tracking and category-level object pose tracking. In both situations,  $\mathcal{P}_n$  means rotation  $\mathcal{R} \in SO(3)$  and translation  $\mathcal{T} \in R^3$ . The object size does not need to be estimated, because it can be directly inferred from the initial pose  $\mathcal{P}_0$ . Similarly, in some autonomous driving-related works, pitch and roll do not need to be estimated. During tracking, CAD models of the target instances can be used in the instance level object pose tracking task but are not allowed to be used in the category level object pose tracking task.

## 2.2 Metrics Definition

**2D Projection metric** [23] computes the mean distance between the projections of CAD model points after being transformed by the estimated object pose and the ground-truth pose respectively. A pose is considered correct if the distance between two projections is less than 5 pixels. This metric is suitable for evaluating augmented reality-related algorithms. Since the CAD model of the target object is required to compute projections, the 2D projection metric is only suitable for evaluating instance-level pose detection or tracking methods.

**$n^\circ n$  cm metric** [24] measures whether the rotation error is less than  $n^\circ$  and whether the translation error is below  $n$  cm. If both are satisfied, the pose is considered correct. For symmetrical objects,  $n^\circ n$  cm is computed as the smallest error for all possible ground-truth poses. The most commonly used threshold settings include  $5^\circ 5$  cm,  $5^\circ 10$  cm and  $10^\circ 10$  cm. This metric is suitable for evaluating both

instance-level methods and category-level methods. Mean Average Precision (mAP) at  $n^{\circ}n$  cm (mAP@ $n^{\circ}n$  cm) is often reported in category-level methods.

**ADD metric** [15], [25] computes the mean distance between two transformed model points using the estimated pose and the ground-truth pose. When the distance is less than 10% of the model's diameter, it is claimed that the estimated pose is correct. For symmetric objects, ADD metric is often replaced by ADD-S metric, where the mean distance is computed based on the closest point distance. When models trained on datasets like YCB video [26] are evaluated, the ADD(-S) AUC (Area Under Curve) should also be computed as a metric. The ADD(-S) is also only suitable for evaluating instance-level object pose detection or tracking methods.

**3D Intersection over Union (3DIoU) metric** [27]–[29] also known as 3D Jaccard index, measures how close the predicted bounding boxes are to the ground-truths. Here, the predicted bounding boxes and ground-truths can be easily computed using the predicted and ground-truth object poses along with the object size or the CAD model. Metric 3DIoU takes the predicted box and the ground truth box as input and computes the intersection volume of the two boxes. The final 3DIoU value is equal to the volume of the intersection of two boxes divided by the volume of their union. Therefore, 3DIoU is a normalized metric and its value ranges from 0 to 1. 3DIoU is suitable for evaluating both instance level methods and category level methods. In most of the existing works, mAP@IoU25, mAP@IoU50 and mAP@IoU75 (i.e. if the 3DIoU is higher than 0.25, 0.5 or 0.75 respectively, the predicted pose is regarded as correct) are the most frequently reported indicators.

### 3 DATASETS FOR MONOCULAR OBJECT POSE DETECTION AND TRACKING

Up to now, object pose detection and tracking has developed into a huge and important research field. Progress of deep learning-based object pose detection and tracking is inseparable from the use and construction of many large-scale datasets that are both challenging and credible. In this section, we introduce commonly used mainstream monocular object pose detection and tracking-related datasets. Here, we categorize them into ones for instance-level object pose detection/tracking, and ones for category-level object pose detection/tracking according to whether CAD models of objects are available and whether there exists multi-instance for each category. An overview and a full comparison of these datasets are shown in Table 2, and visualization examples are shown in Figure 3.

#### 3.1 Datasets for Instance Level Object Pose Detection and Tracking

**Linemod** [15] is the most standard benchmark for instance-level object pose detection. It consists of 13 RGBD sequences. Each sequence contains around 1.2k images with ground-truth 6Dof poses (3 degrees for rotation and 3 degrees for translation) of each single target object. The resolution of each image is  $640 \times 480$ . For most of studies, around 15% of images of each sequences are selected for training and the

remaining 85% are selected for testing. Each sequence includes challenging cluttered scenes, texture-less objects and light condition variations, bringing difficulties for accurate object pose prediction. Though containing sequences, the dataset is always only used for object pose detection rather than tracking, as the sequences are short and the train/test split has made them non-continuous.

**Linemod Occlusion** [14] is generated from Linemod dataset to make up for the fact that it lacks occlusion cases. It consists of 1214 RGBD images belonging to *benchwise* sequence of Linemod, where ground-truth 6Dof poses of another 8 severely occluded visible objects are annotated additionally. In most works, Linemod Occlusion is only used for testing models trained on Linemod.

**YCB video** [26] consists of 21 objects collected from YCB object set [33]. The 21 objects are selected due to their high-quality 3D models and good visibility in depth. There are 92 videos in the entire YCB video dataset, and each video is composed of 3 to 9 YCB objects, which are captured by a real RGBD camera. All videos in the dataset consist of 133,827 images. The resolution of each image is  $640 \times 480$ . Varying lighting conditions, significant image noise, and severe occlusions make it challenging to detect object pose in this dataset. Since it is made up of videos, this dataset can be used for both instance-level object pose detection and instance-level object pose tracking. Commonly, 80 videos are used for training, and 2,949 key frames extracted from the rest 12 videos are used for testing.

**T-LESS** [30] is an RGBD dataset with texture-less objects. The dataset consists of 30 electrical parts that have no obvious texture, distinguishable color, or unique reflection characteristics, and usually have similar shapes or sizes. Images in T-LESS are captured by three synchronized sensors: a structured light sensor, an RGBD sensor, and a high-resolution RGB sensor. It provides 39K RGBD images for training and 10K for testing. Images with different resolutions are provided in the dataset. Specifically, there are 3 kinds of resolution ( $400 \times 400$ ,  $1900 \times 1900$ ,  $720 \times 540$ ) for RGBD images and 1 kind of resolution ( $2560 \times 1920$ ) for RGB images. Backgrounds of images in the training set are mostly black, while the backgrounds of images in the test set vary a lot, including different lighting, occlusion, etc. The texturelessness of objects and the complexity of environments make it a challenging dataset.

**HomebrewedDB** [31] contains 33 highly accurately reconstructed 3D models of toys, household objects and low-textured industrial objects (specifically, 17 toy, 8 household, and 8 industry-relevant objects) of sizes varying from 10.1 to 47.7 cm in diameter. The dataset consists of 13 sequences from different scenes, each containing 1340 frames filmed using 2 different RGBD sensors. All data are collected from scenes that span a range of complexity from simple (3 objects on a plain background) to complex (highly occluded with 8 objects and extensive clutter). Precise 6Dof pose annotations are provided for dataset objects in the scenes, obtained using an automated pipeline. Since data are collected by different sensors, resolutions of images are quite different in some ways. For instance, both color and depth images in the sequences recorded by Carmine sensor have a default resolution of  $640 \times 480$ , while images collected by Kinect are kept a size of  $1920 \times 1080$  in the final.

Datasets	Levels	Format	Num_Categories	CAD models	Annotation	Resolution	Scale	Usage
Linemod [15]	Instance	RGBD	13	Yes	6Dof	640 × 480	15k	detection
Linemod Occlusion [14]	Instance	RGBD	8	Yes	6Dof	640 × 480	1.2k	detection
YCB video [26]	Instance	RGBD	21	Yes	6Dof	640 × 480	134k	detection & tracking
T-LESS [30]	Instance	RGBD	30	Yes	6Dof	-	49k	detection
HomebrewedDB [31]	Instance	RGB	33	No	6Dof	-	17k	detection & tracking
KITTI3D [27]	Category	RGB	8	No	7Dof	384 × 1280	15k	detection
ApolloScape [32]	Category	RGB	3	Yes	9Dof	2710 × 3384	5k	detection
NOCS(CAMERA275) [28]	Category	RGBD	6	Yes	9Dof	640 × 480	300k	detection
NOCS(REAL25) [28]	Category	RGBD	6	Yes	9Dof	-	8k	detection
Objectron [29]	Category	RGB	9	No	9Dof	1020 × 1440	4M	detection & tracking

TABLE 2  
A comparison of datasets for monocular object pose detection and tracking.

Texturelessness, scalability changes, occlusion changes, light conditions changes, and object appearance changes together constitute the complexity of this dataset.

### 3.2 Dataset for Category Level Object Pose Detection and Tracking

KITTI3D [27] is the most widely used dataset used for category level monocular object pose detection. The most commonly used data split is 7481 RGB images for training and 7518 RGB images for testing. All images are annotated with 7 degree of freedom (7Dof) label: three for object translation, three for object size, and one for object rotation. A total of 8 object categories are annotated, and the most commonly evaluated 3 categories are *car*, *pedestrian* and *cyclist*. The resolution of each image is  $384 \times 1280$ . Strictly speaking, due to the lack of annotations for pitch and roll, we cannot fully recover the 9Dof pose of objects using models trained on this dataset. However, because its application scenario is about autonomous driving and 7Dof information is rich enough for this task, this dataset has received extensive attention. In KITTI3D, only annotations of training split are publicly available, and evaluation scores on test split can only be obtained by submitting prediction results to the official website [benchmark website](#). Each image in KITTI3D is provided with a corresponding point cloud, collected by a LiDAR, which is broadly used for 3D object detection. Since this paper only reviews works for monocular object pose detection, works about utilizing point clouds for 3D object detection on KITTI3D will not be reviewed.

*ApolloScape* [32] is originally released for the *ApolloScape 3D Car Instance challenge*. The released dataset contains a diverse set of stereo video sequences recorded in street scenes from different cities. There are 3941/208/1041 high-quality annotated images in the training/validation/test set. The resolution of each monocular RGB image is  $2710 \times 3384$ . The annotations are 9 degrees of freedom (9Dof). Therefore, compared with KITTI3D, ApolloScape is more suitable for evaluating performances of category object pose detection related models. Another advantage of this dataset is that car models are provided. In total, 79 car models belong to three categories (sedan1, sedan2, SUV), and only 34 models appear in training set.

*NOCS* [28] is now the most famous dataset for category-level object pose detection. It consists of the synthetic CAMERA275 dataset and the real-world REAL25 dataset. A total of 6 categories are involved in NOCS. For CAMERA275, 300K composited images are rendered, among which 25K

are set aside for validation. Totally, 184 instances selected from ShapeNetCore and 31 widely varying indoor scenes (backgrounds) [34] are used for rendering. For REAL25, 8K RGBD frames (4300 for training, 950 for validation, and 2750 for testing) of 18 different real scenes (7 for training, 5 for validation, and 6 for testing) are captured. In NOCS, the resolution of each image is  $640 \times 480$ . For each training and testing subsets, 6 categories and 3 unique instances per category are used. For the validation set, 6 categories with 1 unique instance per category are used. More than 5 object instances are placed in each scene to simulate real-world clutter. CAD models of instances are available for both CAMERA275 and REAL25. All test images have been annotated with 9Dof parameters w.r.t pose and size. The fly in the ointment is that object poses and sizes in training datasets are roughly obtained through registering, which are not as accurate as test annotations.

*Objectron* [29] dataset is a collection of short object-centric video clips, accompanied by AR session metadata, including camera poses, sparse point clouds, and characterization of the planar surfaces in the surrounding environment. In each video, the camera moves around the object, capturing it from different views. This dataset also contains manually annotated 3D bounding boxes for each object, which describe the object's position, orientation, and dimensions. Objectron consists of 15K annotated video clips supplemented with over 4M annotated images belonging to categories of bikes, books, bottles, cameras, cereal boxes, chairs, cups, laptops, and shoes. The original resolution of each image is  $1920 \times 1440$ . In addition, to ensure geo-diversity, this dataset is collected from ten countries across five continents. Due to the richness of this dataset, it is very suitable for evaluating the performance of category-level monocular object pose detection/tracking methods, especially when only RGB data is used. The disadvantage is that most images contain only one object, and it occupies most of the image area, which is not conducive to training some object pose detection or tracking models for robot grasping. But for AR scenarios, this dataset is simply a boon for the industry.

## 4 INSTANCE LEVEL MONOCULAR OBJECT POSE DETECTION

Instance level monocular object pose detection aims to detect the object of interest and estimate its 6Dof pose (i.e. 3D rotation  $\mathcal{R} \in SO(3)$  and 3D translation  $\mathcal{T} \in R^3$ ) relative to a canonical frame. Particularly, the CAD model

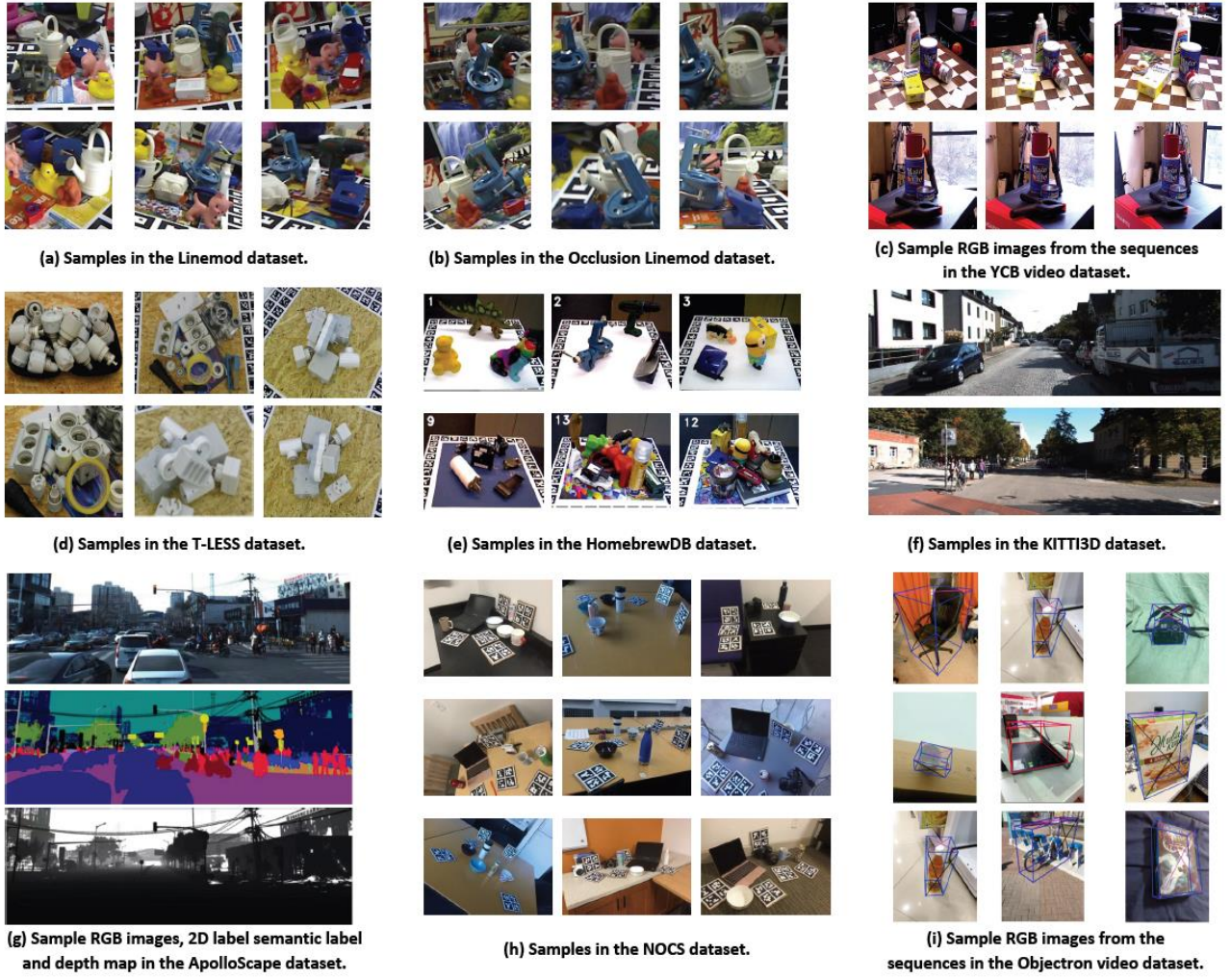


Fig. 3. Image examples of commonly used datasets.

of the interested object is available during both training and testing. According to different input data formats, hereby we classify instance-level monocular object pose detection methods into RGB-based methods and (RGB)D-based methods.

#### 4.1 RGB-based Methods

To estimate the 6Dof pose, the most direct way is to let the deep learning model predict pose related parameters directly. However, directly estimating the 6Dof pose from a single RGB image is an ill-posed problem and faces challenges. Thanks to the existence of CAD models, establishing 2D-3D correspondences between the input image and object model can help ease the task. According to the above observation, we provide an overall schematic representation of RGB-based instance-level monocular object pose detection methods in Figure 4. In general, we divide deep learning based methods into five major classes: direct methods, keypoint-based methods, dense coordinate based methods, refinement-based methods and self-supervised methods.

**Direct methods.** One of the most intuitive ways to predict the 6Dof pose is to treat object pose estimation as a regression or classification task, and directly predict object pose related parameter presentations (for example, Euler angles or quaternions for rotations) from input images. For instance, Xiang et al. [26] introduce a novel deep learning model for end-to-end 6Dof pose estimation named PoseCNN, which decouples object pose estimation task into several different components. For translation estimation, PoseCNN firstly localizes the 2D object center in the image and estimates the depth w.r.t the camera. The 3D translation can be recovered according to the projection equation. For 3D rotation, it is estimated by regressing a quaternion representation. Both components have utilized geometric priors to simplify the task. SSD-6D [35] is another direct prediction pipeline. It extends the 2D SSD [36] architecture to 6Dof pose estimation. Instead of regressing rotation parameters continuously, they discretize the rotation space into classifiable viewpoint bins and treat rotation estimation as a classification problem. Recently, Trabelsi et al. [37] put forward a pose proposal network for 6Dof object pose esti-

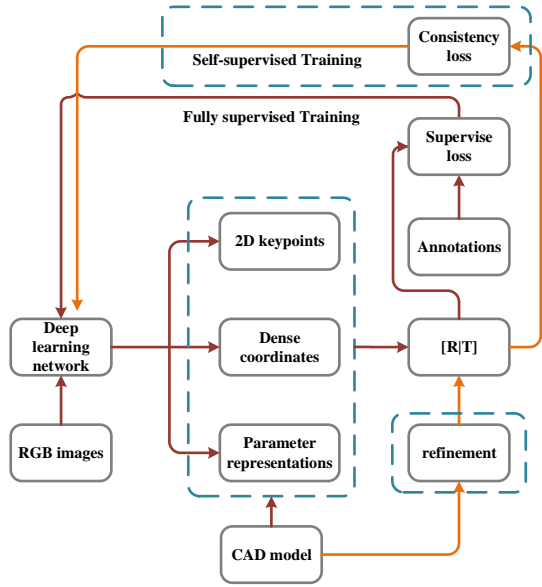


Fig. 4. Overall schematic representation of RGB-based instance level monocular object pose detection methods.

mation. In their work, a CNN-based encoder/multi-decoder module is presented. The multi-decoder decouples rotation estimation, translation estimation, and confidence estimation into different decoders. Hence, specific features can be learned for each subtask. Though intuitive, all the above-mentioned three kinds of methods are highly dependent on time-consuming pose refinement operation to improve performance. In contrast to them, the recent work Efficient-Pose [38] introduces a direct pose estimation framework based on the state-of-the-art EfficientDet [39] architecture. By utilizing the novel 6D augmentation strategy, Efficient-Pose has achieved superior performance without refinement. However, as it is an ill-posed problem, direct methods always perform poorly or can't generalize to natural scenes well. Currently, the better and more popular choice is to establish 2D-3D correspondences and solve them to predict pose related parameters, which will be introduced in the next several subsections. Recently, another branch of works [40]–[42] attempt to adopt such ideas in direct predicting methods. More specifically, they try to modify the indirect methods to direct methods by utilizing neural networks to establish 2D-3D correspondences directly and simulating the Perspective-n-Point (PnP) [43] algorithm using deep learning networks. In this way, the object pose can be directly regressed by the correspondence-extraction network combined with the PnP network. For example, GDR-Net [42] first regresses geometric features using a ResNet [44] backbone to build 2D-3D correspondences. Then, the 2D-3D correspondences are fed to a Patch-PnP solver consisting of CNNs and fully connected layers to predict object pose. The whole framework of GDR-Net can be trained end-to-end. Though requiring 2D-3D correspondences, the object pose can be directly predicted by a network. Thus, this line of works are also regarded as a direct method in this paper.

**Keypoint-based methods.** As mentioned before, compared to directly predicting pose related parameters, build-

ing 2D-3D correspondences for object pose detection is more accurate. Among current correspondence-based methods, keypoint-based methods use CNNs to detect 2D keypoints in the image and then solve a Perspective-n-Point (PnP) problem [43] for pose estimation. As the pioneer, BB8 [45] first uses a deep network to coarsely segment out the object and then use another network to predict 2D projections of the 3D bounding box corners to build 2D-3D correspondences. Based on such 2D-3D correspondences, the 6Dof pose can be estimated by solving the PnP problem. Due to its multi-stage pipeline, BB8 can't be trained end-to-end and is time-consuming for inference. Similar to BB8, Tekin et al. [46] adopt the idea of YOLO [47] framework for 2D detection and extends it for 6Dof object pose detection, namely YOLO-6D. The key component of YOLO-6D is a single-shot deep network that takes the image as input and directly detects the 2D projections of 3D bounding box corners, followed by a PnP solver to estimate object pose. This two-stage pipeline yields a fast and accurate 6Dof pose prediction without requiring any post-processing. After that, this kind of two-stage pipeline methods are adopted by many works [48]–[51], addressing different challenges like occlusion and truncation. For instance, Oberweger et al. [50] propose to predict the 2D projections of 3D keypoints in the form of 2D heatmaps. Comparing to directly regressing coordinates of 2D keypoints, localizing keypoints from heatmaps addresses the issue of occlusion to some extent. However, since heatmaps are fix-sized, it is difficult to handle truncated objects, because some of their keypoints may be outside the image. To solve this problem, PVNet [52] adopts the strategy of voting-based keypoint localization. Specifically, they first train a CNN to regress pixel-wise vectors pointing to the keypoints, i.e., vector field, and then use the vectors belonging to the target object pixels to vote for keypoint locations. Thanks to this vector-field representation, the occluded or truncated keypoints can be robustly recovered from the visible parts, enabling PVNet to yield good performance under severe occlusion or truncation. Inspired by PVNet, some works also perform a pixel-wise voting scheme for keypoint localization to improve performance. For instance, Yu et al. [53] propose an effective loss on top of PVNet to achieve more accurate vector-field estimation by incorporating the distances between pixels and keypoints into the objective. Then, HybridPose [54] extends unitary intermediate representation to a hybrid one, which includes keypoints, edge vectors, and symmetry correspondences. This hybrid representation exploits diverse features to enable accurate pose prediction. However, regressing more representations also causes more computational cost and limits inference speed.

**Dense coordinate based methods.** Beyond keypoints, another kind of correspondence-based methods are dense coordinate based methods, which formulate the 6Dof object pose estimation task as building dense 2D-3D correspondences, followed by a PnP solver to recover the object pose. The dense 2D-3D correspondences are obtained by predicting the 3D object coordinate of each object pixel or predicting dense UV maps. Before deep learning becomes popular, early works usually use random forest for predicting object coordinates [14], [55], [56]. Then Brachmann et al. [23] extend the standard random forest to an auto-

context regression framework, which iteratively reduces the uncertainty of the predicted object coordinate. However, the performances of these early works are poor, because random forest can only learn limited features in simple scenarios. To handle more complicated conditions, recent studies introduce deep learning networks to predict 3D coordinates of object pixels. For instance, CDPN [57] is a pioneer work in adopting deep learning models for dense coordinates prediction. In CDPN, the predicted 3D object coordinates are used to build a dense correspondence between 2D image and 3D model, which has shown robustness towards occlusion and clutter. However, CDPN neglects the importance of handling symmetries. To accurately estimate the 6Dof pose of symmetric objects, Pix2Pose [58] builds a novel loss function, namely transformer loss, which can transform the predicted 3D coordinate of each pixel to its closest symmetric pose. The above-mentioned methods all directly regress dense 3D object coordinates, which is also an ill-posed problem and may face challenges for continuously predicting. Instead of directly regressing 3D coordinates, DPOD [59] builds 2D-3D correspondences by means of UV maps. Given a pixel color, its corresponding position on the 3D model surface can be estimated based on the correspondence map, thus providing a relation between image pixels and 3D model vertices. Moreover, regressing UV maps turns out to be a much easier task for the network. The above methods, whether to predict coordinates or UV maps, make predictions for all visible points on the object, which is inefficient and difficult to learn. While in EPOS [60], the target object is represented by compact surface fragments, and correspondences between densely sampled pixels and the fragments are predicted using an encoder-decoder network, which is much more efficient and geometrically more reasonable. Besides, by doing so, challenging cases like objects with global or partial symmetries can be solved to a certain degree.

In summary, dense coordinate based methods have shown their robustness to heavy occlusions and symmetries. Still, regressing object coordinates is more difficult than predicting sparse keypoints due to the larger continuously searching space.

**Refinement-based methods.** You may notice that we have mentioned that some methods require a refinement step to improve their performances. Here, we call these methods refinement-based methods, which estimate the object pose by aligning synthetic object renderings with scene images. This kind of method may overlap with some methods that have mentioned above. But because they are usually the key to improving the prediction performance, we also introduce them separately here.

Given an initial pose estimation, DeepIM [61] exploits a deep learning-based pose refinement network to iteratively refine the initial pose by minimizing the differences between the observed image and the rendered image under the current pose. The refined pose is then used as the initial pose for the next iteration, until the refined pose converges or the number of iterations reaches a threshold. Similarly, Manhardt et al. [62] also adopt the iterative matching pipeline and propose a new visual loss that drives the pose update by aligning object contours. Moreover, DPOD [59] develops a standalone pose refinement network including

three separate output heads for regressing rotation and translation. In the work of Trabelsi et al. [37], the attention mechanism is integrated into a deep network for refining the initial pose by highlighting important parts. The above-mentioned methods focus on comparing the rendered image and the observed image, ignoring the importance of realistic rendering. Recently, Yen-Chen et al. [63] propose a framework iNeRF to invert an optimized neural radiance field for rendering and has achieved promising results.

These refinement networks have already been integrated into some instance-level object pose detection models to produce more accurate results. For example, PoseCNN [26] is combined with DeepIM [61]. However, the speed of refinement-based methods depends heavily on the number of iterations and the used renderer, which becomes a bottleneck for their popularization.

**Self-supervised methods.** In the 6Dof object pose detection task, current deep learning models highly rely on training on annotated real-world data, which are hard to obtain. An intuitive way is to use cost-less synthetic data for training. Nevertheless, it has been proven in many works that models simply trained on synthetic data demonstrate poor generalization ability towards real-world scenarios due to the vast domain gap between synthetic and natural data.

Therefore, domain randomization (DR) [69] is proposed and used [64]. Its core idea is to generate enormous images by sampling random object poses and placing the model on random background images. In this way, the real world domain is only a subset of the generated domain so that the model can learn as much 6Dof pose related features as possible through utilizing these synthetic images. In addition, many methods [70] attempt to generate more realistic renderings [28], [70], [71] or use data augmentation strategies [38], [52].

These schemes, however, can not address the challenges like severe occlusions, and the performance on real data is still far from satisfactory. In this context, the idea of self-supervised learning is introduced. For instance, Deng et al. [72] propose a novel robot system to label real-world images with accurate 6D object poses. By interacting with objects in the environment, the system can generate new data for self-supervised learning and improve its pose estimation results in a life-long learning fashion. Recently, Self6D [65] leverages the advances in neural rendering [73] and proposes a self-supervised 6Dof pose estimation solution. Self6D first trains the network on synthetic data in a fully supervised manner, and then fine-tunes it on unlabeled real RGB data through a self-supervised manner by seeking a visually and geometrically optimal alignment between real and rendered images. Similarly, Sock et al. [66] propose a two-stage 6Dof object pose estimator framework. In their work, the first stage enforces the pose consistency between rendered predictions and real input images, narrowing the gap between these two domains. The second stage fine-tunes the previously trained model by enforcing the photometric consistency between pairs of different object views, where one image is warped and aligned to match the view of the other, thus enabling their comparison. Additionally, the above introduced iNeRF [63] has no need to use any real annotated data for training. Therefore, it also belongs to this

Methods	Types	Input	Pose refinement	2D projection metric	ADD(-S) metric	5 °5 cm metric
Brachmann et al.(2016) [23]	Dense	RGB	Yes	73.7	50.2	40.6
BB8(2017) [45]	Keypoints	RGB	Yes	89.3	62.7	69.0
SSD-6D(2017) [35]	Direct	RGB	Yes	-	76.3	-
PoseCNN(2017) [26]	Direct	RGB	No	70.2	62.7	19.4
DeepIM(2018) [61]	Refinement	RGB	Yes	97.5	88.6	85.2
YOLO-6D(2018) [46]	Keypoints	RGB	No	90.37	55.95	-
Sundermeyer et al. [64]	Self-supervised	RGB	No	-	28.65	-
Pix2Pose(2019) [58]	Dense	RGB	No	-	72.4	-
PVNet(2019) [52]	Keypoints	RGB	No	99.00	86.27	-
CDPN(2019) [57]	Dense	RGB	No	98.10	89.86	94.31
DPOD(2020) [59]	Dense	RGB	Yes	-	95.15	-
Yu et al. (2020) [53]	Keypoints	RGB	No	99.40	91.50	-
HybridPose(2020) [54]	Keypoints	RGB	Yes	-	91.30	-
Self6D(2020) [65]	Self-supervised	RGB	No	-	58.9	-
iNeRF(2020) [63]	Self-supervised	RGB	Yes	-	79.2	-
Sock et al. [66]	Self-supervised	RGB	No	-	60.6	-
Li et al. (2020) [67]	Self-supervised	RGB	No	-	80.4	-
EfficientPose(2021) [38]	Direct	RGB	No	-	97.35	-
Trabelsi et al.(2021) [37]	Direct	RGB	Yes	99.19	93.87	-
GDR-Net(2021) [42]	Direct	RGB	No	-	93.7	-
DSC-PoseNet(2021) [68]	Self-supervised	RGB	No	-	58.6	-

TABLE 3  
Perfomance of instance level RGB-based methods on Linemod dataset.

Methods	Types	Input	Pose refinement	2D projection metric	ADD(-S) metric	5 °5 cm metric
PoseCNN(2017) [26]	Direct	RGB	No	17.2	24.9	-
DeepIM(2018) [61]	Refinement	RGB	Yes	56.6	55.5	30.9
YOLO-6D(2018) [46]	Keypoints	RGB	No	6.16	6.42	-
Oberweger et al. (2018) [50]	Keypoints	RGB	No	60.9	30.4	-
Pix2Pose(2019) [58]	Dense	RGB	No	-	32.0	-
SegDriven(2019) [51]	Keypoints	RGB	No	44.9	27.0	-
PVNet(2019) [52]	Keypoints	RGB	No	61.06	40.77	-
DPOD(2020) [59]	Dense	RGB	Yes	-	47.25	-
Yu et al. (2020) [53]	Keypoints	RGB	No	-	43.52	-
Single-stage(2020) [40]	Direct	RGB	No	62.3	43.3	-
HybridPose(2020) [54]	Keypoints	RGB	Yes	-	47.5	-
Self6D(2020) [65]	Self-supervised	RGB	No	-	32.1	-
Sock et al. [66]	Self-supervised	RGB	No	-	22.8	-
Li et al. (2020) [67]	Self-supervised	RGB	No	-	42.3	-
GDR-Net(2021) [42]	Direct	RGB	No	-	62.2	-
Trabelsi et al.(2021) [37]	Direct	RGB	Yes	65.46	58.37	-
DSC-PoseNet(2021) [68]	Self-supervised	RGB	No	-	24.8	-

TABLE 4  
Perfomance of instance level RGB-based methods on the Occlusion Linemod dataset.

Methods	Types	Input	Pose refinement	2D projection metric	ADD(-S) metric	ADD(-S) AUC metric
PoseCNN(2017) [26]	Direct	RGB	No	3.7	21.3	61.3
DeepIM(2018) [61]	Refinement	RGB	Yes	-	-	81.9
Oberweger et al. (2018) [50]	Keypoints	RGB	No	39.4	-	72.8
SegDriven(2019) [51]	Keypoints	RGB	No	30.8	39.0	-
PVNet(2019) [52]	Keypoints	RGB	No	47.4	-	73.4
Single-stage(2020) [40]	Direct	RGB	No	48.7	53.9	-
GDR-Net(2021) [42]	Direct	RGB	No	-	60.1	84.4
Li et al. (2020) [67]	Self-supervised	RGB	No	15.6	-	50.5

TABLE 5  
Perfomance of instance level RGB-based methods on the YCB-Video dataset.

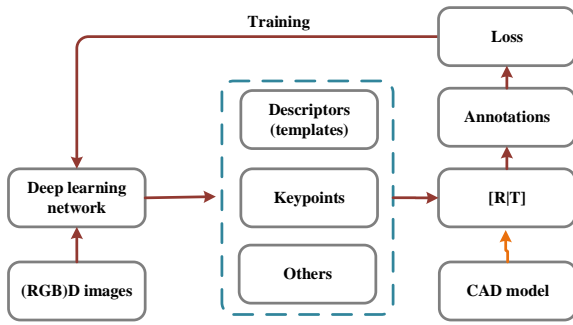


Fig. 5. Overall schematic representation of (RGB)D-based instance level monocular object pose detection methods.

line of work. Beyond leveraging image-level consistency for self-supervised learning, inspired by recent keypoint-based methods [52], [54], DSC-PoseNet [68] develops a weakly-supervised and self-supervised learning based pose estimation framework, where a weakly-supervised segmentation method and a self-supervised keypoints learning method are developed to enforce dual-scale keypoints consistency without using pose annotations. Recently, Li et al. [67] use the consistency between an input image and its DR augmented counterpart to achieve self-supervised learning. As a result, this self-supervised framework can robustly and accurately estimate the 6Dof pose in challenging conditions and ranks the best self-supervised based instance-level monocular object pose detection model.

Till now, we have introduced most of the recent state-of-the-art RGB based instance level monocular object pose detection methods from several different perspectives. And we give full performance comparisons of most of these above-mentioned methods in Table 3, Table 4, and Table 5 on Linemod dataset, Occlusion Linemod dataset, and YCB-Video dataset, respectively.

## 4.2 (RGB)D-based Methods

RGB images lack depth information, making the 6Dof object pose detection task an ill-posed problem. Fortunately, the development of monocular RGBD camera motivates the (RGB)D-based 6Dof pose estimation methods. (RGB)D-based methods take RGBD images or depth masks as input and predict object pose by making full utilization of the power of the point cloud presentation. In general, the (RGB)D-based methods can be classified into retrieval-based methods, keypoints-based methods and other deep learning based methods. An overall schematic representation of (RGB)D-based instance-level monocular object pose detection methods is shown in Figure 5.

**Retrieval-based methods.** A direct solution of predicting object pose is to traverse all possibilities. We can first generate a dataset of (RGB)D images covering all possible object poses using CAD model. Then we can retrieve the most similar image of the target object from the dataset to determine the object pose given an observed RGBD image or depth mask. The retrieval can be achieved by comparing image descriptors or matching templates. In this paper, we call this kind of methods as retrieval-based methods.

Traditional methods [15], [82]–[85] achieve retrieving or template matching by using hand-craft features, therefore owning limited perception power. Motivated by traditional retrieval-based methods, to the best of our knowledge, Kehl et al. [86] are the first to propose to train a CAE (Convolutional Auto Encoder) [87] from scratch using RGBD patches to learn descriptors for retrieval. When new RGBD images come, the target object poses can be predicted by matching object descriptors with these descriptors in the codebook. Though large improvements have been obtained compared to traditional methods, the work of Kehl et al. [86] faces challenges in handling occlusion and texture-less objects. Therefore, Park et al. [88] put forward Multi-Task Template Matching (MTTM). MTTM only uses depth masks as input to find the closest template of the target object. In this pipeline, object segmentation and pose transformation are performed in the meantime to remove irrelevant points. By eliminating irrelevant points, MTTM shows great robustness in pose estimation. It is worth mentioning that MTTM has the potential of being generalized to category level since both object segmentation and pose transformation are instance-independent. However, the performance of MTTM decreases largely without using CAD models. In contrast to the above methods that directly learn descriptors or templates relying on the network architecture itself, some methods introduce triplet comparison in their pipelines for learning more powerful descriptors. For example, Alexander et al. [89] propose a deep learning based descriptor predicting method using triplet loss, which successfully untangles different objects and views into clusters. Then, based on this work [89], Balntas et al. [90] further develop a new descriptor representation that enforces a direct relationship between the learned features and pose label differences to better represent object pose in the latent space. Next, Zakharov et al. [91] draw an angular difference function and set a constant angle threshold as dynamic margin into triplet loss to obtain faster training as well as better performance.

In summary, retrieval-based methods can achieve robust performance in most cases. However, they need to discrete the rotation space for defining codebooks, which would cause rough prediction when the discrete interval is large and computational in-efficiency when the discrete interval is small.

**Keypoints-based methods** Similar to RGB-based methods, in RGB(D)-based methods, there are also a line of works that attempt to predict object pose by extracting object keypoints. This kind of methods always construct 3D-3D correspondence to solve object pose utilizing predicted keypoints. PVN3D [76] may be the first deep learning work that successfully estimates object pose by extracting 3D keypoints. A deep Hough voting network is designed to detect 3D keypoints of objects and then estimate the 6D pose parameters within a least-squares fitting manner. Then, PointPoseNet [92] combines the advantage of both color and geometry information to improve PVN3D. Specifically, PointPoseNet simultaneously predicts segmentation mask and regresses point-wise unit vectors pointing to the 3D keypoints. Then unit vectors of segmented points are used to generate the best pose hypothesis with the help of geometry constraints. Both PVN3D and PointPoseNet choose to use keypoints selected by Farthest Point Sampling

Method	Type	Year	Input	Pose Refinement	LINEMOD [15]	YCB video [26]
DenseFusion [74]	Other	2019	RGB-D	Yes	-	96.8
MoreFusion [75]	Other	2020	RGB-D	Yes	-	95.7
PVN3D [76]	Keypoints	2020	RGB-D	No	95.5	-
PVN3D [76]+ICP	keypoints	2020	RGB-D	Yes	96.1	-
Gao et al. [77]	Other	2020	Depth	Yes	-	82.7
Gao et al. [77]+ICP	Other	2020	Depth	Yes	-	76.0
G2L-Net [78]	Other	2020	RGB-D	No	98.7	92.4
CloudAAE [79]	Other	2021	Depth	No	82.1	-
CloudAAE [79]+ICP	Other	2021	Depth	Yes	92.5	93.5
RCVPose [80]	Keypoints	2021	RGB-D	No	99.4	95.2
RCVPose [80]+ICP	Keypoints	2021	RGB-D	Yes	99.7	95.9
FFB6D [81]	Keypoints	2021	RGB-D	No	99.7	97.0
FFB6D [81]+ICP	Keypoints	2021	RGB-D	No	-	96.6

TABLE 6  
Performance comparison of (RGB)-D based instance level monocular 6Dof pose detection methods.

(FPS). In contrast, FFB6D (Full Flow Bidirectional fusion network designed for 6D pose estimation) [81] comes up with a novel keypoint selection algorithm called SIFT-FPS in replacement of FPS to fully leverage texture and geometry information. SIFT-FPS formulates two steps. In the first step, SIFT [93] features are extracted to extract 2D keypoints. In the second step, 2D keypoitns are transformed into 3D and further selected by FPS. In this way, the selected keypoints could be more evenly distributed on object surface and be more texture distinguishable. More recently, Wu et al. [80] argue that previous vector or offset schemes are sensitive to disperse keypoints and therefore propose model RCV-Pose. In RCV-Pose, the radial voting scheme is introduced, where for each object point, a deep learning model is used to learn several spheres. Each keypoint may locate on the surface of a sphere. Therefore, during inference, the algorithm only needs to use the surface of these spheres to vote for a 3D accumulator space, and peaks of which indicate keypoint locations. Compared to previous methods, RCV-Pose only needs to predict 3 keypoints, which is much more efficient.

**Other methods.** In addition to the methods mentioned above, numbers of works have also shown great interest in designing models that satisfy some special requirements beyond pursuing accuracy. First, some methods have made attempts to solve problems caused by complex scenarios like occlusion and clutter. For instance, Alexander et al. [94] propose an approach that “learns to compare” the observed RGBD image and the rendered image to better handle occlusion and complicated sensor noise, which is achieved by describing the posterior density of a particular object pose with a convolutional neural network (CNN) that compares observed and rendered images. Jafari et al. [95] present a three-step decomposition approach with the help of instance segmentation and dense coordinate regression to handle occlusion, known as the first deep learning-based accurate pose estimator for partly occluded objects. Then, Wang et al [74] propose DenseFusion, which fully leverages color and depth information, leading to robustness in heavy occlusion and changing lighting conditions. Furthermore, MoreFusion [75] performs pose prediction with surrounding spatial awareness, and joint multiple-object pose optimization, which greatly promotes consistency and accuracy of pose estimation in cluttered scenes with heavy occlusion and contracting objects. Second, besides handling complex scenarios, recent studies have shown interest in designing

more lightweight network architectures to prompt real-time performance. The work of Gao et al. [77] is known as the first point cloud only based deep learning 6Dof pose estimation method. Since only point cloud is required to be processed, the network architecture proposed by Gao et al. [77] is much more lightweight than methods that take both RGB data and depth data as input. Then, Chen et al. [96] use segmented object point cloud patches from the target object’s CAD model as input and form a pose prediction model without the need for fine-tuning, thus saving computational cost. Additionally, G2L-Net [78] decouples the prediction pipeline into global localization, translation localization, and rotation localization and estimates object pose through a coarse-to-fine manner without using a CAD model, achieving real-time performance. Third, in addition to care about running time, Gao et al. [79] improve the generalization ability of models trained on synthetic data. They argue that domain gap between real and synthetic is considerably smaller and easier to fill for depth information. Therefore, they present an end-to-end 6Dof pose prediction architecture called CloudAEE, which utilizes an augmented autoencoder and a lightweight depth data synthesis pipeline to cooperatively improve generalization ability.

Till now, we have introduced most of recent state-of-the-art (RGB)D-based instance-level monocular object pose detection methods. And we give a full performance comparison of keypoints based methods and other methods in Table 6. The metric is ADD(-S). Since retrieval-based methods don’t use commonly used datasets or unified experimental settings, we don’t quantitatively compare them in this survey.

## 5 CATEGORY LEVEL MONOCULAR OBJECT POSE DETECTION

In this section, we introduce category-level monocular object pose detection methods. According to whether the prediction focuses on 1Dof rotation or 3Dof rotation, we classify related methods into Category Level Monocular 3D Object Detection and Category Level Monocular 6D Pose Detection.

### 5.1 Category Level Monocular 3D Object Detection

Category level monocular 3D object detection needs to predict 7 degrees of freedom (7Dof) pose configurations,

Methods	Types	Types	Depth Estimation	[val/val2/test] Easy	[val/val2/test] Moderate	[val/val2/test] Hard
Mono3D [97]	2016	Others	No	2.53 / - / -	2.31 / - / -	2.31 / - / -
Deep3Dbox [98]	2017	2D proposal	No	5.85 / - / -	4.10 / - / -	3.84 / - / -
GS3D [99]	2019	2D proposal	No	13.46 / 11.63 / 4.47	10.97 / 10.51 / 2.90	10.38 / 10.51 / 2.47
FQNet [100]	2019	2D proposal	No	5.98 / 5.45 / 2.77	5.50 / 5.11 / 1.51	4.75 / 4.45 / 1.01
ROI-10D [101]	2019	2D proposal	No	10.12 / - / -	1.76 / - / -	-1.30 / - / -
MonoGRNet [102]	2019	2D proposal	No	13.88 / - / 9.61	10.19 / - / 5.74	7.62 / - / 4.25
MonoDIS [103]	2019	2D proposal	No	18.05 / - / 10.37	14.96 / - / 7.96	13.42 / - / 6.40
M3D-PRN [104]	2019	2D proposal	No	20.27 / 20.40 / 14.76	17.06 / 16.48 / 9.71	15.21 / 13.34 / 7.42
SMOKE [105]	2019	Keypoints	No	- / 14.76 / 14.03	- / 12.85 / 9.76	- / 11.50 / 15.28
Jorgensen et al. [106]	2019	Keypoints	No	14.52 / 9.45 / 11.74	13.15 / 8.42 / 9.58	11.85 / 7.34 / 7.77
Pseudo-LiDAR [107]	2019	Psudeo-LiDAR	Yes	28.2 / - / -	18.5 / - / -	16.4 / - / -
Mono3D-PliDAR [108]	2019	Psudeo-LiDAR	Yes	31.5 / - / 10.76	21.0 / - / 7.50	17.5 / - / 6.10
AM3D [109]	2019	Psudeo-LiDAR	Yes	32.23 / 28.31 / 16.50	21.09 / 15.76 / 10.74	17.26 / 12.24 / 9.52
DA-3Ddet [110]	2020	Psudeo-LiDAR	Yes	33.4 / - / 16.8	24.0 / - / 11.5	19.9 / - / 8.9
PatchNet [111]	2020	Psudeo-LiDAR	Yes	35.1 / 31.6 / 15.68	22.0 / 16.8 / 11.12	19.6 / 13.8 / 10.17
D4LCN [112]	2020	Psudeo-LiDAR	Yes	26.97 / 24.29 / 21.71	24.0 / 19.54 / 11.72	18.22 / 16.38 / 9.51
FADNet [113]	2020	Keypoints	No	23.98 / - / 16.37	16.72 / - / 9.92	16.72 / - / 8.05
MoNet3D [114]	2020	Keypoints	No	22.73 / - / -	16.73 / - / -	15.55 / - / -
RTM3D [115]	2020	Keypoints	No	20.77 / - / 14.76	16.86 / - / 9.71	16.63 / - / 7.42
UR3D [116]	2020	Others	Yes	28.05 / 26.30 / 15.58	18.76 / 16.75 / 8.61	16.55 / 13.60 / 6.00
RAR-Net [117]	2020	Others	No	23.12 / - / 16.37	19.82 / - / 11.01	16.19 / - / 9.52
kinematic3D [118]	2020	Others(video)	No	- / - / 19.07	- / - / 12.72	- / - / 9.17
Li et al. [119]	2021	Keypoints	No	22.50 / 22.71 / 16.73	19.60 / 17.71 / 11.45	17.12 / 16.15 / 9.92
Liu et al. [120]	2021	Others	Yes	23.63 / - / 16.65	16.16 / - / 13.25	12.06 / - / 9.91
CaDDN [121]	2021	Psudeo-LiDAR	Yes	23.57 / - / 19.17	16.31 / - / 13.41	13.84 / - / 11.46
OCM3D [122]	2021	Psudeo-LiDAR	Yes	23.65 / - / 17.48	17.75 / - / 10.44	15.93 / - / 7.87
Peng et al. [123]	2021	Psudeo-LiDAR	Yes	26.17 / - / 22.73	19.61 / - / 14.82	15.93 / - / 12.88

TABLE 7  
Perfromance of category level monocular 3D object detection methods on KITTI3D dataset.

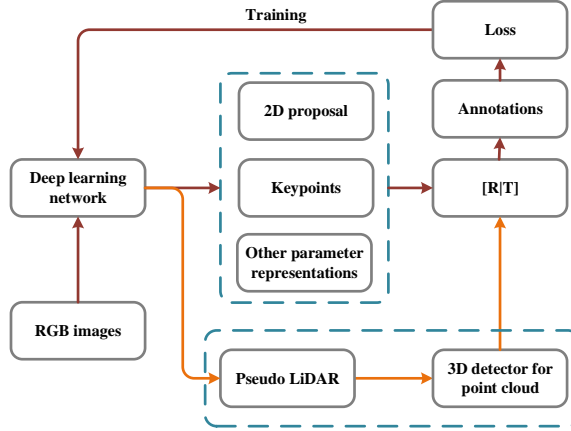


Fig. 6. Overall schematic representation of category level monocular 3D object detection methods.

including rotation  $\mathcal{R} \in SO(1)$  (i.e. only yaw needs to be predicted), translation  $\mathcal{T} \in R^3$  and object size  $\mathcal{S} \in R^3$ . There are no CAD models available during training and testing. Category-level monocular 3D object detection is of great significance to autonomous driving scenarios. It is more concerned about the accuracy of translation prediction, while the accuracy of rotation prediction can be relaxed accordingly. Point clouds collected by LiDAR and monocular RGB images are the most commonly used data formats. Since this paper focuses on *monocular* object pose detection, the former is out of the scope of this paper, and we refer readers to [124]–[126] for a detailed introduction. An overall schematic representation of category-level monocular 3D object detection methods that take RGB images as input is

shown in Figure 6.

To the best of our knowledge, Mono3D [97] is the first deep learning method that achieves this goal. It focuses on generating 3D object proposals by using instance segmentation, object contour, and ground-plane assumption. However, the ground-plane assumption is not always held in some scenarios, and utilizing so many auxiliary supervision signals to train a model would burden the model during training.

**2D proposal based methods.** Soon, Deep3Dbox [98] is proposed as an external state-of-the-art object detector to generate 2D proposals and process the cropped proposals within a deep neural network to estimate 3D dimensions and orientation. In Deep3Dbox, the relationship between the predicted 2D boxes and the projected 3D boxes on the image plane is exploited (by aligning projections of 3D box corners with lines of corresponding 2D boxes) in post-optimization to help calculate 3D parameters. It is to say that the 3D box can not be predicted in an end-to-end manner using the deep learning network, which is a certain limitation. Next, GS3D [99] leverages the off-the-shelf 2D object detector Faster-RCNN [127] to obtain a coarse cuboid using each predicted 2D box as guidance, hence achieving end-to-end training. Though being an end-to-end framework, GS3D highly relies on the assumption that the top center of the object 3D box has a stable projection on the 2D plane (i.e., it is very close to the top midpoint of the 2D box), and so does the bottom center of the 3D box. The assumption is, however, not strictly mathematical reasonable. M3D-PRN [104] is proposed to use the depth-aware convolution to generate 2D and 3D object proposals simultaneously, and use 2D-3D geometric constraints as post-processing to improve precision. In M3D-RPN, 2D anchors and 3D anchors are bounded according to some geometric constraints (for

example, for 3D anchors of the same size, their corresponding 2D boxes satisfy the law of near-large and far-small.) to obtain better prediction results. However, pre-defining 2D-3D bounded anchors is a difficult problem, and it is difficult to exhaust all possibilities. FQNet [100] is proposed to infer 3D IoU between the predicted 3D box and ground-truth box to further predict the most likely candidate 3D bounding box. Therefore, FQNet has the ability to learn and reason about 3D spatial relationships from 2D projections. However, image patches should be cropped and resized in FQNet's pipeline, which is not efficient, especially when there are plenty of objects in an image. In contrast, ROI-10D [101] is more direct as it directly utilizes features of Region-of-Interest (RoI) to lift 2D detection to 3D, and no image patch cropping process is required. The above introduced methods all predict 3D boxes by leveraging their relationship with the corresponding 2D bounding boxes. While MonoGRNet [102] directly optimizes the 3D box in an end-to-end manner and achieves accurate 3D object detection by fusion of 2D detection, instance depth estimation, 3D location estimation, and local corner regression. The depth estimation in MonoGRNet refers to only predicting the depth of centers of 3D bounding boxes, therefore, no additional ground-truth depth maps are needed as labels to train the network, making the application scope of the scheme not limited by requiring additional annotation cost. At the same time, MonoDIS [103] discovers that isolating the group parameters during training would benefit the network. Inspired by this observation, MonoDIS is trained by disentangling the 3D parameters into rotation, translation, and object size, and isolated loss functions are used to supervise learning. More importantly, the disentangling training mode can be integrated into any monocular 3D object detection model.

**Keypoints based methods.** The above mentioned methods incorporate a 2D proposal network as the base architecture, which causes the bottlenecks of inference time. Instead, SMOKE [105] is proposed to directly predict the 3D keypoints of object 3D bounding boxes through a concise single-stage framework. Then, FADNet [113] improves SMOKE by using several ConvGRU layers [128] to learn parameters related to calculate 3D keypoints. Besides, it suggests to learn depth hint vector to better perceive the depth difference between different pixel rows, which coincides with the idea of depth-convolution in M3D-RPN. The drawback of FADNet is that its network structure is too large, making it hard to achieve real-time performance. MoNet3D [114] is also a keypoint-based method. It is highly dependent on the assumption that if two objects are horizontally close in the image and have the same depth, they are also very close in 3D space. Instead of directly predicting 3D keypoints, RTM3D [115] first predicts 2D keypoints and then uses geometric constraints to lift and refine 2D keypoints to 3D box-related parameters. Compared with previous methods, RTM3D has achieved a great improvement in both accuracy and speed. Unfortunately, the post lifting and refinement process is not differentiable, making it impossible to implement end-to-end prediction. Recently, Li et al. [119] successfully solve the problem by designing a differentiable refinement module that can predict precisely 3D boxes. Similar to RTM3D, Jorgensen et al. [106] decompose the 3D

box and the 2D box into 26 predictors. After predicting these 26 parameters, the rough 3D bounding box are obtained first. Then a least square algorithm is used to refine the 3D bounding box, with 3D IoU as the best optimization target. However, the least square algorithm they use is also not differentiable.

**Pseudo-LiDAR methods.** Unlike previous RGB image-based methods, the concept of pseudo-LiDAR is proposed by PL-MONO (Pseudo-LiDAR) [107] that introduces depth information into 3D object detection. Instead of directly estimating 3D bounding boxes from the scene, pseudo-LiDAR predicts the depth  $Z(u, v)$  of each image pixel  $(u, v)$ . The resulting depth map  $Z$  is then projected into a 3D point cloud, and a pixel  $(u, v)$  is transformed to  $(x, y, z)$  by

$$z = Z(u, v), x = \frac{(u - c_u) \times z}{f_u}, y = \frac{(v - c_v) \times z}{f_v}$$

where  $(c_u, c_v)$  is the camera center and  $f_u$  and  $f_v$  are the horizontal and vertical focal lengths. The pseudo-LiDAR points can then be regarded as LiDAR signals, and any off-the-shelf LiDAR-based 3D object detectors can be applied to them. By making use of state-of-the-art depth estimation algorithms, the simple yet effective PL-MONO (Pseudo-LiDAR) method, has achieved promising improvement on the monocular 3D object detection task benchmarked on KITTI3D dataset. Although PL-MONO (Pseudo-LiDAR) has greatly promoted monocular 3D object detection performance, there is still a significant performance gap between pseudo-LiDAR and real LiDAR. Afterwards, Weng and Kitan [108] propose model Mono3D-PLiDAR and point out that the detection performance of the current method is severely limited by the noise in pseudo-LiDAR data. Guided by the observed misleading and long-tail issues in the noisy pseudo-LiDAR, a 2D-3D bounding box consistency loss is proposed as an additional supervision signal in Mono3D-PLiDAR to solve the problem. Meanwhile, Pseudo-LiDAR++ [129] reckons that the quality of depth estimation plays an important part in pseudo-LiDAR related methods, especially for the depth accuracy of faraway objects. Therefore, a stereo network architecture, as well as corresponding loss functions are designed to better estimate the depth of faraway objects. Next, E2E-PLiDAR [130] is proposed as an end-to-end pipeline based on differentiable Change of Representation (CoR) modules that allow back-propagation throughout all layers, preserving the modularity and compatibility of pseudo-LiDAR. The above-mentioned methods all rely on off-the-shelf 3D object detectors for predicting 3D bounding boxes. While Ma et al. [111] analyze the effect of depth data representation on performances and discover that the performance improvement comes from the 3D coordinates representation rather than 3D detectors. They propose PatchNet, which improves performance over previous pseudo-LiDAR models by integrating the 3D coordinates as additional channels of input data. In essence, PatchNet attempts to improve detection performance from the perspective of obtaining better representations, while authors of DA-3Ddet [110] attempt to solve the problem of learning more precise features. In DA-3Ddet, the feature from the image-based pseudo-LiDAR domain is adapted to the real LiDAR domain, contributing to a novel domain adaptation-based monocular 3D object

detection framework. A Context-Aware Foreground Segmentation (CAFS) module is also introduced in DA-3Ddet to solve the inconsistency between the foreground mask of pseudo-LiDAR and real LiDAR caused by inaccurately estimated depth. In contrast to the methods mentioned above that focus on improving depth feature quality or representation quality, authors of AM3D [109] claim that RGB features from the original image also shouldn't be ignored. Therefore, they improve the representation of the point cloud by adopting a multi-modal features fusion module to integrate complementary RGB features into the pseudo-LiDAR pipeline. Reading et al. [121] also research how to combine image features in CaDDN, where Bird's-Eye-View (BEV) images are used. Specifically, they use a predicted categorical depth distribution for each pixel to project rich contextual feature information to the appropriate depth interval in 3D space, and then combine a BEV projection and single-stage detector to produce the final detection results. The above methods all focus on learning better features, while Ding et al. [112] investigate how to learn better convolutional kernels in D4LCN. They propose a new Local Convolutional Network (LCN). Instead of learning global kernels to apply to all images, the convolutional kernels are automatically learned from image-based depth maps and locally applied to each pixel and channel of individual image sample, narrowing the gap between image and 3D point cloud. Recently, Simonelli [131] observes that the validation results published by existing pseudo-LiDAR based methods are substantially biased. As a result, mechanism for predicting a 3D confidence score is further introduced to address the problem. Then, authors of OCM3D [122] again find that current methods can't handle the noisy nature of the monocular pseudo-LiDAR point cloud. Therefore, they propose to build voxels for each object proposal, allowing the noisy point cloud to be organized effectively within a voxel grid, to improve performance. Nearly at the same time, Peng et al. [123] argue that implicit utilizing LiDAR point clouds to train depth estimation models can't fully explore their capabilities and consequently lead to sub-optimal performances. To tackle this, they directly use real LiDAR point clouds to guide the training of monocular 3D detectors rather than use re-predicted depth, which significantly improves the performance. Note that, in Peng et al. [123], real LiDAR point clouds are only required during training, the same as training a depth estimator.

**Other methods.** Beyond the above methods, Shi et al. [116] propose a Distance-Normalized Unified Representation (DNRU) in model UR3D to help the model learn a unified representation for objects at different depths. However, their method requires estimating pixel depth to construct the DNRU simultaneously, and most of the detection accuracy gains come from the estimated depth, which is not effective and efficient. Liu et al. [120] introduce a method that can leverage the ground information as priors. It removes non-ground anchors to reduce redundancy and votes the ground pixel below the current pixel to learn geometric cues. Although it is intuitive, it is not easy to vote for ground pixels, especially when interference factors such as occlusion exist. Besides, it also needs to predict depth map for improving performance. In addition to the monocular 3D detection method that we define as taking

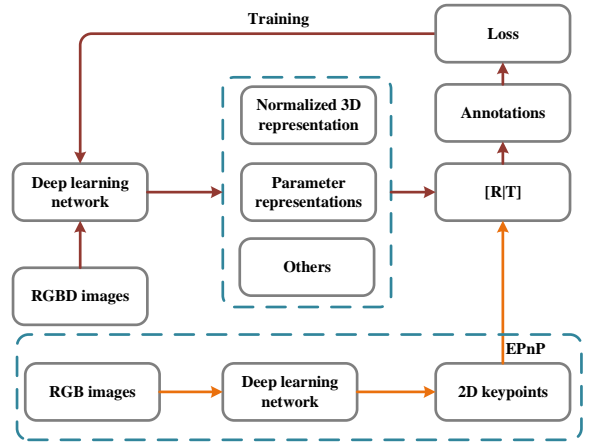


Fig. 7. Overall schematic representation of category level monocular 6D pose detection methods.

a single image as input, Brazil et al. [118] propose model kinematic3D, which leverages 3D kinematics from monocular videos to improve the overall localization precision of the monocular 3D object detection task. It also produces useful scene dynamic by-products (i.e. ego-motion and per-object velocity) that benefit autonomous driving. Beyond methods focusing on designing end-to-end network architectures, A post-optimization that can be integrated into any monocular detectors. is proposed in RAR-Net [117]. This method starts with an initial 3D box prediction and then refine it gradually towards the ground truth, with only one 3D parameter changed in each step. The progress is optimized by reinforcement learning. The limitation is RAR-Net requires optimization for multi-steps, which increases additional computational cost.

Till now, we have introduced the recent state-of-the-art monocular 3D object detection methods. Table 7 presents an overview and a full comparison of representative works. The results are about the performance of these methods on KITTI val1, val2, and test split respectively. We report the mAP@IoU75 of *Car* class, which is the most widely concerned category in monocular 3D object detection. The results about val1 split and val2 split are reported using the  $mAP_{11}@IoU70$  metric to provide a complete comparison for all published related works. And the results about test split are reported using the  $mAP_{40}@IoU70$  metric, which is the latest standard evaluation metric of KITTI's official leader-board.

## 5.2 Category Level Monocular 6D Pose Detection

In category level monocular 6D pose detection task, we need to predict 9 degrees of freedom (9Dof) pose configurations including rotation  $\mathcal{R} \in SO(3)$ , translation  $\mathcal{T} \in R^3$  and object size  $\mathcal{S} \in R^3$ . There is no CAD model available to help ease the estimation task. Strictly speaking, it should be named as 9Dof object pose detection. To conform to the customary convention, we still call it category level monocular 6D pose detection in this survey. The main challenge of this task is how to endow the model with the ability to deal with intra-class variation [137]. Compared to category-level

Data	Methods	Input	To pose	mAP@IoU25	mAP@IoU50	mAP@5°5cm	mAP@10°5cm	mAP@10°10cm
CAMERA25	NOCS(2019) [28]	RGBD	Aligning	91.4	85.3	38.8	61.7	62.2
	SPD(2020) [132]	RGBD	Aligning	93.2	83.1	59.0	73.3	81.5
	CASS(2020) [133]	RGBD	Regressing	-	-	-	-	-
	CPS(2020) [134]	RGBD	Regressing	29.0	8.7	-	-	31.7
	CPS+ICP(2020) [134]	RGBD	Aligning	90.2	70.4	42.8	-	63.8
	DualPoseNet(2021) [135]	RGBD	Regressing	92.4	86.4	70.7	77.2	84.7
REAL275	NOCS(2019) [28]	RGBD	Aligning	84.9	80.5	9.5	26.7	26.7
	SPD(2020) [132]	RGBD	Aligning	77.3	53.2	21.4	43.2	54.1
	CASS(2020) [133]	RGBD	Regressing	84.2	77.7	23.5	58.0	58.3
	CPS(2020) [134]	RGBD	Regressing	48.9	19.2	-	-	14.7
	CPS+ICP((2020)) [134]	RGBD	Realigning	84.5	72.6	25.8	-	28.6
	DualPoseNet(2021) [135]	RGBD	Regressing	79.8	62.2	35.9	50.0	66.8
	FS-Net(2021) [136]	RGBD	Regressing	95.1	92.2	28.2	60.8	64.6

TABLE 8  
Performance of category level monocular 6D pose detection methods on NOCS dataset.

monocular 3D object detection task, this task requires the model to predict another 2 degrees of freedom w.r.t rotation. Specifically, we need to predict the pitch angle and roll angle of the object except for the yaw angle. Intuitively, it seems that there is not much difference, but in fact, it is much more difficult to learn the entire  $SO(3)$  space than just learn the  $SO(1)$  space, especially when only RGB image can be used as input.

Sahin et al. [138] are the first to propose the concept of category-level pose estimation. In their work, a part-based Random Forest is introduced, where a category of CAD instances are decomposed into parts and represented with skeletons to train the Random Forest. During inference, parts of an instance are organized in the form of several trees to hypothesize 6Dof poses. Their method highly relies on the geometric characters of a category/instance. Therefore, it mainly deals with depth input. Besides, the dataset they mainly focus on is quite simple and is limited to an ideal environment (instance images with no background). What's more, their work is not a deep learning method.

**Detecting by aligning.** Then, Wang et al. [28] introduce a shared canonical representation for all possible object instances within a category named Normalized Object Coordinate Space (NOCS), which, strictly speaking, is the first deep learning method for category level monocular 6D pose detection. In Wang et al. [28], the RGBD patch of the target object is first segmented using the detection results of an off-the-shelf 2D object detection/segmentation method Mask-RCNN [139]. Then the patch is learned to predict the NOCS representation using a region-based neural network. After that, the 6Dof pose and object size can be recovered using the Umeyama algorithm [140] by aligning the predicted NOCS in the camera coordinate system to the canonical NOCS in the object coordinate system. Another contribution of Wang et al. [28] is that they have released the NOCS dataset (including CEMERA25 and REAL275), which is now the most widely used benchmark for category level monocular 6D pose detection. Wang et al.'s work [28] performs well, however, inferring the object pose by only predicting the NOCS presentation is actually not an easy task for the reason that intra-class variation is so large. Therefore, SPD [132] is proposed to handle the intra-class variations by learning a deformation field from the pre-learned shape prior. Meanwhile, SPD infers the dense correspondences between the depth observation of the object instance and the

reconstructed 3D model to jointly estimate the 6Dof object pose and size. Though it improves the performance, SPD still needs the Umeyama [140] post-optimization algorithm and can not predict the poses of objects in an end-to-end manner. Besides, it is hard for them to generalize to RGB-only scenarios.

**Detecting by regressing.** Appropriately, Chen et al. [133] propose CASS, where a canonical shape space that models the latent space of canonical 3D shapes with a normalized pose is learned to tackle intra-class shape variations. In their model, shape-dependent features and pose-dependent features are contrasted and fused to directly regress the object pose and size. Another model that directly regress 6Dof pose and size is CPS [134], which predicts 6Dof pose and size using Region of Interests (RIO) features after RoI Align [139]. In CPS, a shape encoding is learned to recover the point cloud using a PointNet [141] decoder. By doing so, the features learned by the encoder network can be improved with additional supervision during training. However, the performance of CPS is poor if it directly predicts the pose and size without using ICP as a refinement. More recently, DualPoseNet [135] is proposed to further improve the performance of detecting by regressing methods. The improvement of DualPoseNet comes from the used Spherical Convolution [142] and its dual Explicit-Implicit Pose Decoder architecture. The Spherical Convolution is used to learn  $SO(3)$  equivalent representations so that the rotation can be recovered easier using features learned from it. The Explicit Decoder and the Implicit Decoder are used to directly predict pose/size and reconstruct canonical point cloud representation of the target object, respectively. Then, a refinement algorithm is proposed in DualPoseNet by considering the consistency between the Explicit Decoder and the Implicit Decoder. Besides DualPoseNet, Chen et al. [136] recently propose FS-Net to directly predict object pose and size too. In FS-Net, an orientation-aware autoencoder with 3D graph convolution is used for latent feature extraction. The 3D graph convolution is scale and translation invariant. Therefore, features learn from it is only aware of rotation. Thus, rotation recovered from it would be more precise. And it recovers the scale and size by learning residuals between the scale and size of the reconstructed point cloud and the ground-truth, which reduces research space and hence eases the task. It is worth mentioning that Chen et al. [136] propose a 3D Deformation Mechanism(3DM) in their work.

They generate new training examples by enlarging, shrinking, or changing the area of some surfaces of the box-cages to deform rigid objects, which increases the abundance of intra-class variations and prompts the model to learn more discriminative features. Detecting by regressing methods demonstrates the potential of being extended to RGB-only scenarios. However, few effort has been paid towards this direction.

**Detecting by keypoints.** The above-mentioned models consist of the recently state-of-the-art category level monocular 6D pose detection methods. However, they share a common drawback, which is they all mainly focus on utilizing RGBD data as input, limiting their application scenarios, especially for applications such as Augmented Reality(AR) on mobile phones due to the difficulty in obtaining depth information. Besides, complex network architecture and time-consuming post-optimization also make it difficult for them to achieve real-time performance. Therefore, MobilePose [143] is proposed. MobilePose is built upon the light-weight MobileNet v2 [144]. It predicts the 2D keypoints of the object in the image. Note that it only takes RGB images as input. Then, the up-to-scale 9Dof object bounding box is recovered by solving the EPnP [43] problem. Lately, Ahmadyan et al. [29] release the Objectron dataset they used and introduce MobilePose v2, a two-stage category-level 6D pose detection pipeline built upon MobilePose. In MobilePose v2, SSD [36] is first used to detect 2D object patches in the image. Then, detected patches are cropped and resized and are input into an EfficientNet-like [145] network to predict 2D keypoints. Then the same EPnP algorithm is used as done in MobilePose to recover the up-to-scale 9Dof object bounding box. Both MobilePose and MobilePose v2 can achieve real-time performance and have the potential of being applied to terminals such as mobile phones. Since they mainly focus on serving for AR, the final solutions are up-to-scale (i.e., they cannot estimate the absolute depth of the object from the camera), which may be the main drawback of this kind of methods.

**Other Methods.** In addition to the above discussed major kinds of methods, some methods focus on designing more general solutions or handling more challenging cases. For example, Chen et al. [146] propose to use an analysis-by-synthesis strategy for category level 6D pose detection. Specifically, they propose a gradient-based fitting procedure with a parametric neural image synthesis module to implicitly represent the appearance, shape, and pose of entire object categories and rendering can be achieved without CAD models. The pose can be predicted by comparing the decoded image and the observed real image. Though this method achieves the goal of only taking RGB data as input, the performance drops significantly when depth information is not available. Besides, it may be sensitive to initialization and be time-consuming due to refining for multiple iterations. In contrast to predicting the pose of rigid objects, Li et al. [147] propose Articulation-aware Normalized Coordinate Space Hierarchy (ANCSH) – a canonical representation for different articulated objects in a given category for detecting object pose of articulated objects. The task involved in this work requires the model to predict per part 6D poses, 3D scales, joint parameters (i.e., type, position, axis orientation), and joint states (i.e., joint angle).

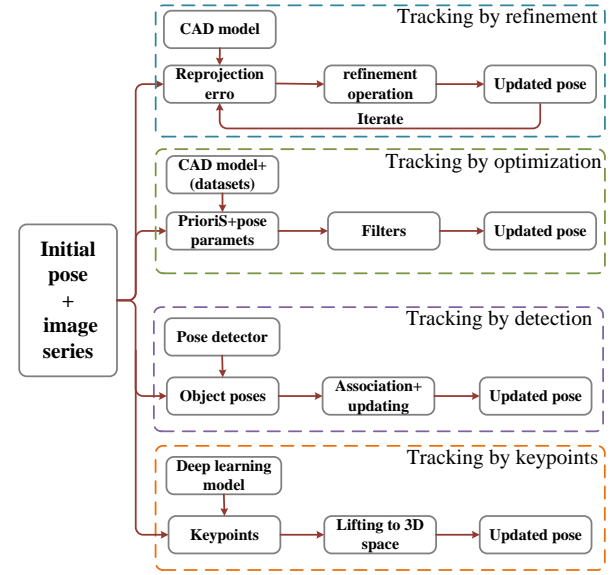


Fig. 8. Overall schematic representation of monocular object pose tracking.

Although ANCSH has achieved good results only by using depth information, how to use the more feature-rich RGB information has not been studied in this work.

Till now, we have introduced the recent state-of-the-art monocular category level monocular 6D pose detection methods. The above methods are mostly benchmarked on NOCS dataset (CEMERA25 and REAL275) with the evaluation metrics mAP@IoU25, mAP@IoU50, mAP@5°5cm, mAP@10°5cm, mAP@10°10cm to joint measure performances. Their main results on RGBD data are reported in Table 8. We also report results of MobilePose and MobilePose v2 on Objectron dataset in Table 9. The evaluation metric is mAP@IoU50.

## 6 MONOCULAR OBJECT POSE TRACKING

In this section, we introduce monocular object pose tracking methods. According to whether CAD models are available, we classify related methods into Instance Level Monocular Object Pose Tracking and Category Level Monocular Object Pose Tracking. An overall schematic representation of monocular object pose tracking is shown in Figure 8.

### 6.1 Instance Level Monocular Object Pose Tracking

Instance level monocular object pose tracking requires us to predict 6 degrees of freedom(6Dof) pose of a sequence of images (i.e., a video). The pose parameters include rotation  $\mathcal{R} \in SO(3)$  and translation  $\mathcal{T} \in R^3$ . Similar to instance level monocular object pose detection task, CAD models of target objects are available and the object size  $\mathcal{S} \in R^3$  is not required to be regressed. The difference is that an initial pose of the first frame is given in instance level object pose tracking.

**Tracking by refinement.** To the best of our knowledge, Deep 6-DOF Tracking (D6DT) [148] is the first work

Methods	Input	How to pose	bike	book	bottle	camera	cereal_box	chair	cup	laptop	shoe
MobilePose(2020) [143]	RGB	EPnP	0.3486	0.1818	0.5449	0.4762	0.5496	0.7112	0.3722	0.5548	0.423
MobilePose v2(2020) [29]	RGB	EPnP	0.6127	0.5218	0.5744	0.8016	0.6272	0.8505	0.5388	0.6735	0.6606

TABLE 9  
Performance of category level monocular 6D pose detection methods on NOCS dataset.

that leverages deep learning for 6D pose tracking, which takes RGBD sequences of real objects as input. D6DT is a rendering-based method. It first uses the pose of the last frame in the sequence to render a synthetic RGBD frame for the target object. Then the rendered image and the currently observed image are input into a deep learning network for predicting the relative 6Dof object pose between these two input frames. Then, marougkas et al. [149] improve D6DT by integrating multiple parallel soft spatial attention modules into the network architecture to handle background clutter and occlusion. Both D6DT and marougkas et al. [149] require RGBD data as input, while DMB6D [62], which adopts the same idea as D6DT, only takes RGB images as input. In DMB6D, a new visual loss is proposed to drive the pose update process. It works by aligning object contours in the image, hence avoiding using any explicit appearance model and depth information for solving the pose. In essence, all the three methods are implemented by means of pose refinement,i.e., they use pose of the last frame as an initialization of the current frame, and then use neural networks to refine the initial pose. Since they do refinement simply through one single forward pass, the final predicted pose is somehow coarse. In contrast, DeepIM [61] is proposed to iteratively refine the pose by matching the rendered image against the observed image. The relative pose between the rendered image and the observed image is predicted by a FlowNet [150] like network during each iteration. Though achieving good performance, DeepIM needs to use a large amount of real-world observed images to train its network and runs slow at test time. On the contrary, the recently proposed SE(3)-TrackerNet [71] can be trained using synthetic data only, and can achieve real-time performance. The superior performance of SE(3)-TrackerNet mostly comes from the rotation-translation disentanglement scheme, a Lie Algebra rotation representation and the domain randomization data enhancement strategy [69]. Beyond the above methods, Busam et al. [151] propose "I Like to Move It", which learns a decision process to iteratively determine an acceptable final pose. They build a decision process where an initial pose is updated in incremental discrete steps. The model sequentially moves a virtual 3D rendering towards the correct 6D pose solution. "I Like to Move It" is very similar to DeepIM and SE(3)-TrackerNet. The difference is that it is designed on top of reinforcement learning, while the other two models are built upon deep neural networks.

**Tracking by optimization.** In contrast to the above tracking by refinement scheme, PoserBPF [152] achieves object tracking by using a tracking by optimization scheme. Specifically, it combines Rao-Blackwellized particle filtering with a learned auto-encoder network for updating object pose. In PoseRBPF, a Rao-Blackwellized particle filter is used to estimate discredited distributions over rotations and translations. The 3D translation is updated straightforward

by the filter. The rotation is updated by comparing the image descriptor with pre-computed entries in the codebook, generated by an auto-encoder. Though PoseRBPF performs good, the continuous rotation space should be discretized in advance to obtain the codebook, which severely limits the performance of the algorithm. Besides, complexity of the algorithm increases linearly as the number of discretized rotations increases. In addition, Majcher et al. [153] also adopt the idea of particle filtering. In their work, the interested object is segmented by a U-Net in advance. Then, the 6Dof pose of the object in the current frame is estimated by matching the segmented object with the rendered image using the pose of the last frame. The final pose is obtained by optimizing the difference between object silhouettes and edges, during which the particle filter is used to estimate posterior probability distribution. Both PoseRBPF [152] and Majcher et al. [153] work well in clean environment, while they are not suitable for complicated environment such as scenarios where occlusion exists. Therefore, Zhong et al. [154] design a occlusion robust method using a so-called "see through the occluder" scheme, instead of trying to detect the occluder. In Zhong et al.'s study [154], a learning-based video segmentation module is integrated into an optimization-based pose estimation module to form a closed loop so that the "see through" scheme can be achieved. Note, the above tracking by optimization methods are all partially built upon deep learning models and can not achieve end-to-end training and testing.

## 6.2 Category Level Monocular Object Pose Tracking

The same as instance-level object pose tracking, category-level object pose tracking also only requires the model to predict 6 degrees of freedom (6Dof) poses of a sequence of images given the initial pose. The size of the object is not required to be recovered, since it can be determined by the initial pose directly. The difference is that in category level monocular object pose tracking, CAD models are not allowed to be used. Therefore, though methods like DMB6D [62] claim they achieves category level object pose tracking, we don't classify them as category-level in this paper, as they use CAD models of instances in their works.

**Tracking by detection.** To the best of our knowledge, Mono3D-tracking [155] is the first work that defines the category level 3D vehicle bounding box tracking problem and proposes to jointly track and detect vehicles in 3D from a series of monocular RGB images. Specifically, given a series of images, it first detects 2D bounding boxes of objects to generate proposals for each image. Then features of proposals are used to predict independent 3D layout (i.e., depth, orientation, dimension, a projection of 3D center). After that, proposals of different frames are associated and refined leveraging the so-called occlusion-aware association and depth-ordering matching strategy. Mono3D-tracking achieves tracking by exploring image features, while 3DOT

[156] straightforwardly incorporates a 3D Kalman filter [157] into this task. And Hungarian algorithm [158] is used in 3DOT for state estimation and data association. More specifically, in 3DOT [156], 3D bounding boxes are generated from a series of images by an off-the-shelf 3D object detector. Then, a 3D Kalman filter is used to update the factorized parameters of these 3D boxes frame by frame. Note that in their original paper, the 3D bounding boxes are detected from LiDAR point clouds. However, 3D bounding boxes detected from monocular RGB/RGBD images can also be used since the detecting stage and tracking stage are independent in 3DOT. Therefore, we also classify it as a monocular work. The main contribution of 3DOT is that it provides a baseline and new evaluation metrics for object pose tracking. Similar to 3DOT, Weng et al. [159] propose to use LSTM and Graph Convolutional Network to update pose, which shares the same idea with 3DOT. However, simply employing 3D Kalman filter or LSTM would cause the box drifting problem when tracking for a long range. Besides, both 3DOT and Mono3D-tracking can only track 7Dof pose, where the pitch and roll of the object are ignored. In contrast to them, in MotionNet [160], the ignored two angles can also be recovered. MotionNet first detects and segments the target object at the current frame using the object mask of the last frame. Then segmented image patches of both frames are input into a deep network to recover rotation and translation. Among the whole pipeline, LSTM layers [161] and ConvLSTM layers [162] are used to learn sequential information. Compared to other methods, MotionNet performs better in long range.

**Tracking by keypoints.** Unlike the above tracking by detection methods, CenterTrack [163] implements tracking by keypoints scheme that takes a pair of images as input and output object keypoints of the late frame for tracking. It adopts the framework of CenterNet [164]. In CenterTrack, objects are localized and associated with the previous frame by predicting and associating keypoints. Specifically, it takes the image of current frame, the image of last frame and the keypoints of the last frame as input, and predicts object poses of the current frame and keypoint offsets between these two frames. The object pose is tracked end-to-end through a single shot, making the algorithm simple and fast. However, CenterTrack can only track 7Dof object pose. On the contrary, Wei et al. [165] present a system for motion tracking, capable of robustly tracking planar targets and performing relative-scale 6Dof tracking without calibration, which can run in real-time on mobile phones. To track planar targets, given 3D coordinates of 4 objects corners in the previous frame and the corresponding 2D coordinates in the current frame, they solve the rigid body transformation (3D rotation and translation) using a Levenberg-Marquardt optimization algorithm. Later, Ahmadyan et al. [166] improve the work of Wei et al. [165] by tracking the projected 2D coordinates of the 3D bounding boxes' 9 keypoints (8 corners and 1 center). After all keypoints are tracked, the up-to-scale 6Dof pose can be recovered by solving an EPnP problem. Though lightweight and simple, it is obvious that both methods [165], [166] have a common defect: they can only estimate the up-to-scale 6Dof pose, which is enough for AR/VR application while is not enough for robotic grasping or autonomous driving. Therefore, 6-

PACK [167] is proposed, which takes monocular RGBD images as input and estimates object pose by accumulating relative pose changes over time. More specifically, an anchor-based keypoint-generation scheme is first employed to adaptively generate keypoints from the previous frame and the current frame. Then, two sets of ordered keypoints as well as previously computed instance poses are used to obtain the current estimated 6Dof pose. The main limitation of 6-PACK is that it can only work at a situation when depth information is available and can not generalize to RGB-only scenarios.

Till now, we have introduced the recent state-of-the-art monocular object pose tracking methods. Since they focus on different scenarios and taking different data formats as input, it is hard to give a unified quantitative comparison.

## 7 ANALYSIS FOR POSSIBLE FUTURE WORKS AND CHALLENGES

We have introduced the latest developments in monocular object pose estimation from the perspectives of instance-level detection, category-level detection and object pose tracking. Next, to help the community develop this research direction better, we analyze and introduce some possible future research directions and challenges in this section.

**For instance level object pose detection using RGB images only,** we observe that:

- First, though existing algorithms have performed sufficiently well in simple indoor scenarios, they are still difficult to handle situations where occlusion and cluttered backgrounds exist. However, interference like occlusion is inevitable in practical applications. Therefore, studying how to deal with complex interference such as occlusion is a good future research direction.
- Second, existing RGB-only methods are very susceptible to factors such as lighting changes and shooting angles. These factors can cause image blur, reflection, blind spot, cutoff, etc., which may obscure features extracted from images, especially when these features are used for detecting keypoints. This may not be a big deal for environment-controlled indoor scenarios (e.g., indoor factories). However, when it comes to outdoor applications, such as augmented reality on mobile phones, since the lighting condition is uncontrollable and unpredictable, this would become the biggest obstacle for its wide application. Therefore, designing algorithms that are robust to the above factors should also be an important research topic in the future.
- Third, existing researches have shown that establishing 2D-3D correspondences for object pose estimation performs better than directly predicting pose parameters, and mainstream works are long committed to research on how to better establish correspondences. However, this kind of methods can't be trained in an end-to-end manner. Besides, building and solving correspondence is time-consuming.

Therefore, in the future, we need to consider designing differentiable 2D-3D correspondences solving algorithms, replacing it with neural networks, or exploring the possibility of improving the performance of correspondence-free methods.

**For instance level object pose detection using (RGB)D data,** we find:

- Though existing methods always perform much better than RGB-only methods, they often consume much more computational resources since additional depth information needs to be learned. And some methods require additional refinement steps like ICP for performance gain, which further increases running time. Therefore, designing a more lightweight network architecture to reduce both time complexity and space complexity may be a possible valuable future research topic.
- Most existing low power hardware like mobile phones can only capture sparse point clouds in use. While existing (RGB)D-based methods are all evaluated on datasets with dense point clouds generated from depth maps, their performance on sparse point clouds are under-explored. This has caused a bias between evaluating performance and practical use. Therefore, it is necessary to study whether current algorithms are suitable for taking sparse point clouds as input or not. If not, tailored new algorithms should be proposed.
- As we all know, labelling 6Dof pose of objects is very difficult. Therefore, another important challenge we face is how to obtain precise ground-truth poses. Thanks to existing advanced computer graphics technologies, synthetic data with ground-truth is very easy to get and we can use them to train object pose detection models. Nevertheless, models trained on synthetic datasets usually perform poorly on real world images. Therefore, this brings up a new possible future research question: how to improve the generalization ability of models trained on synthetic datasets. Existing self-supervised learning methods have provided some promising pre-researches, but more efforts should be paid. Note that, this research direction is also suitable for both RGB-based instance level methods and category level methods.

In contrast to instance level monocular object pose detection, for category level monocular object pose detection, both category level monocular 3D object detection and category level monocular 6D pose detection are relatively niche.

**For category level 3D object detection,** we observe that:

- As its main application is providing environmental information for autonomous driving, locating objects is more important than predicting the size and orientation of objects. However, locating objects in the 3D space using a single RGB image is ill-posed. Therefore, how to equip the model with the ability of predicting depth is essential. Since images utilized by this task usually contain multiple objects and contain a wide range of feature-rich backgrounds, it

may be a feasible solution to use them to infer depth information. That is to say, how to utilize an instance-aware relationship to improve the model's depth perception ability should be researched, especially for how to utilize non-local features hidden in images. Incorporating Vision Transformers [168], [169] into the network architecture may be a good idea.

- Utilizing Pseudo-LiDAR is a feasible research direction. However, current pseudo-LIDAR-based solutions usually use off-the-shelf depth prediction models to predict depth in advance. It has caused gaps between 3D detection and depth prediction. That is to say, current depth estimation models suffers from the sub-optimal problem, and utilizing Pseudo-LiDAR point clouds generated by them for 3D detection would further aggravate the problem. Therefore, in the future research of pseudo-LiDAR, it may be valuable to combine depth estimation and 3D detection in the same network or in the same training process to obtain mutual performance gain and avoid detection errors accumulated by different sub-optimal problems.
- Existing datasets like KITTI3D always contain both point clouds captured by LiDAR and images captured by monocular camera. Though these point cloud data are not allowed to be used in monocular detection tasks at inference time, it is meaningful to study how to better utilize them for training a monocular 3D object detector. For example, we can utilize point cloud to learn convolutional weights during training while discarding them during inference. Or we can use off-the-shelf point cloud 3D detectors as teacher networks to train monocular 3D detectors, as has been done in knowledge distillation [170], [171].

**For category level monocular 6D pose detection,** we have found that shortcomings of existing methods are obvious:

- Most of the methods need to use an off-the-shelf 2D object detection model to locate the target object in advance. Then the target image patch is cropped out and resized before performing pose prediction. Such a two-stage scheme may cause the accumulation of locating errors. Therefore, a question is if it is possible to generate object proposals and complete pose estimation in a unified network or through a totally proposal-free way. The answer is obviously yes, referring to the successful experience of anchor-free 2D object detection models [164], [172]. However, so far, no researchers have worked in this direction.
- Even though existing methods often use large backbones such as ResNet-101 for learning features to ensure high accuracy and effectiveness, they reduce efficiency meanwhile. Coupled with the time-consuming 2D object detection process, the 6D pose detection architecture is hard to guarantee its real-time performance. Therefore, lightweight real-time performing models are worth studying in the future.
- Most of the existing algorithms are highly dependent on utilizing depth information. However, as

commonly known, taking only RGB image as input is important for many applications like augmented reality on mobile phones. Although there have been proposed several RGB-only methods, the performances of them are poor. Therefore, more efforts can be paid in the direction of RGB-only category-level monocular 6D pose detection.

**For monocular object pose tracking**, we notice that:

- If the CAD model is available, it is not difficult to solve this problem in a controlled scenario. In uncontrollable scenes (such as autonomous driving scenes, outdoor lighting scenes, etc.), we will face all the problems as faced in instance-level object pose detection task.
- We find that existing object pose tracking algorithms usually only take two frames of images (the current frame and one previous frame) as input to predict the object poses of the current frame. This could cause three main problems: first, the sequential information is not fully utilized. Second, tracking errors accumulate over time and cannot be eliminated. Third, the box drift problem may occur. To solve these problems, monocular object pose tracking introduces a feasible future research direction, that is, using recurrent neural networks such as LSTM for associating multi-frame information. It can not only improve the utilization of features but also ensure the stability of the tracking results.
- Many existing methods need to render CAD models, which is time consuming, as most existing renderers are either non-differentiable or cost in-efficient. Therefore, designing efficient and differentiable rendering algorithms is essential in future works.
- In addition, when CAD model is not available, most of the existing works only track 7Dof 3D bounding boxes. To the best of our knowledge, there is only one work [167] that can achieve full 9Dof category-level pose tracking. As mentioned before, 7Dof pose is enough to location-aware scenarios like autonomous driving, while it is not enough for rotation and size-aware scenarios like augmented reality. Therefore, tracking the full 9Dof bounding boxes would be a meaningful future research topic and should be paid more attention.

**For researches on datasets**, attention can be paid on following aspects:

- Considering the difficulty of obtaining real-world ground truth, future studies should focus on designing open-source full 9Dof pose annotation tools, especially tools available on category-level video annotation.
- Most of the existing datasets place codemarkers in the scene when obtaining ground truth poses. These codemarkers provide extra characteristics that would never exist in practical application scenarios. Hence, bias would occur when evaluating and deploying models trained on these datasets. Therefore, real-world datasets that consist of images

without codemarkers should be captured and released.

- For category-level monocular object detection, intra-class variation between instances of the same category in the current dataset NOCS is still limited, i.e., instances are not rich enough, which may make models trained on them hard to generalize to new instance that are quite different to them in appearance. Therefore, the number of distinct instances within the same category should increase for both training and testing to increase intra-class variation for current datasets.
- Although a lot of works have been proposed for tracking, there is still no unified benchmark that can be used to evaluate and compare these algorithms. Therefore, collecting and releasing a large-scale dataset for benchmarking object pose tracking methods is necessary.

## 8 CONCLUSION

This paper presents a contemporary survey of the state-of-the-art deep learning based methods for monocular object pose detection and tracking, including instance level monocular object pose detection, category level monocular object pose detection, and monocular object pose tracking. Metrics and datasets are introduced in detail. Also, a comprehensive taxonomy and performance comparison of these methods are presented both qualitatively and quantitatively. Furthermore, we analyze the potential research directions and challenges in the end.

## REFERENCES

- [1] M. Maurer, J. Christian Gerdes, B. Lenz, and H. Winner, *Autonomous driving: technical, legal and social aspects*. Springer Nature, 2016.
- [2] J. Levinson, J. Askeland, J. Becker, J. Dolson, D. Held, S. Kammler, J. Z. Kolter, D. Langer, O. Pink, V. Pratt *et al.*, "Towards fully autonomous driving: Systems and algorithms," in *2011 IEEE Intelligent Vehicles Symposium (IV)*. IEEE, 2011, pp. 163–168.
- [3] J. Wang, J. Liu, and N. Kato, "Networking and communications in autonomous driving: A survey," *IEEE Communications Surveys & Tutorials*, vol. 21, no. 2, pp. 1243–1274, 2018.
- [4] S. Grigorescu, B. Trasnea, T. Cocias, and G. Macesanu, "A survey of deep learning techniques for autonomous driving," *Journal of Field Robotics*, vol. 37, no. 3, pp. 362–386, 2020.
- [5] J. Tremblay, T. To, B. Sundaralingam, Y. Xiang, D. Fox, and S. Birchfield, "Deep object pose estimation for semantic robotic grasping of household objects," *arXiv preprint arXiv:1809.10790*, 2018.
- [6] K. Bousmalis, A. Irpan, P. Wohlhart, Y. Bai, M. Kelcey, M. Kalakrishnan, L. Downs, J. Ibarz, P. Pastor, K. Konolige *et al.*, "Using simulation and domain adaptation to improve efficiency of deep robotic grasping," in *2018 IEEE international conference on robotics and automation (ICRA)*. IEEE, 2018, pp. 4243–4250.
- [7] S. James, P. Wohlhart, M. Kalakrishnan, D. Kalashnikov, A. Irpan, J. Ibarz, S. Levine, R. Hadsell, and K. Bousmalis, "Sim-to-real via sim-to-sim: Data-efficient robotic grasping via randomized-to-canonical adaptation networks," in *Proceedings of the IEEE/CVF Conference on Computer Vision and Pattern Recognition*, 2019, pp. 12 627–12 637.
- [8] D. Morrison, P. Corke, and J. Leitner, "Closing the loop for robotic grasping: A real-time, generative grasp synthesis approach," *arXiv preprint arXiv:1804.05172*, 2018.
- [9] M.-B. Ibáñez and C. Delgado-Kloos, "Augmented reality for stem learning: A systematic review," *Computers & Education*, vol. 123, pp. 109–123, 2018.

[10] P. Cipresso, I. A. C. Giglioli, M. A. Raya, and G. Riva, "The past, present, and future of virtual and augmented reality research: a network and cluster analysis of the literature," *Frontiers in psychology*, vol. 9, p. 2086, 2018.

[11] M. Gattullo, G. W. Scurati, M. Fiorentino, A. E. Uva, F. Ferrise, and M. Bordegoni, "Towards augmented reality manuals for industry 4.0: A methodology," *robotics and computer-integrated manufacturing*, vol. 56, pp. 276–286, 2019.

[12] J. Peddie, *Augmented reality: Where we will all live*. Springer, 2017.

[13] J. J. Rodrigues, J.-S. Kim, M. Furukawa, J. Xavier, P. Aguiar, and T. Kanade, "6d pose estimation of textureless shiny objects using random ferns for bin-picking," in *2012 IEEE/RSJ International Conference on Intelligent Robots and Systems*. IEEE, 2012, pp. 3334–3341.

[14] E. Brachmann, A. Krull, F. Michel, S. Gumhold, J. Shotton, and C. Rother, "Learning 6d object pose estimation using 3d object coordinates," in *European conference on computer vision*. Springer, 2014, pp. 536–551.

[15] S. Hinterstoisser, V. Lepetit, S. Ilic, S. Holzer, G. Bradski, K. Konolige, and N. Navab, "Model based training, detection and pose estimation of texture-less 3d objects in heavily cluttered scenes," in *Asian conference on computer vision*. Springer, 2012, pp. 548–562.

[16] A. Hornung, K. M. Wurm, and M. Bennewitz, "Humanoid robot localization in complex indoor environments," in *2010 IEEE/RSJ International Conference on Intelligent Robots and Systems*. IEEE, 2010, pp. 1690–1695.

[17] C. Sahin and T.-K. Kim, "Recovering 6d object pose: a review and multi-modal analysis," in *Proceedings of the European Conference on Computer Vision (ECCV) Workshops*, 2018, pp. 0–0.

[18] A. V. Patil and P. Rabha, "A survey on joint object detection and pose estimation using monocular vision," *arXiv preprint arXiv:1811.10216*, 2018.

[19] J. Chen, L. Zhang, Y. Liu, and C. Xu, "Survey on 6d pose estimation of rigid object," in *2020 39th Chinese Control Conference (CCC)*. IEEE, 2020, pp. 7440–7445.

[20] G. Du, K. Wang, and S. Lian, "Vision-based robotic grasping from object localization pose estimation grasp detection to motion planning: A review," *arXiv preprint arXiv:1905.06658*, 2019.

[21] K. Kleeberger, R. Bormann, W. Kraus, and M. F. Huber, "A survey on learning-based robotic grasping," *Current Robotics Reports*, pp. 1–11, 2020.

[22] C. Sahin, G. Garcia-Hernando, J. Sock, and T.-K. Kim, "A review on object pose recovery: from 3d bounding box detectors to full 6d pose estimators," *Image and Vision Computing*, vol. 96, p. 103898, 2020.

[23] E. Brachmann, F. Michel, A. Krull, M. Y. Yang, S. Gumhold *et al.*, "Uncertainty-driven 6d pose estimation of objects and scenes from a single rgb image," in *Proceedings of the IEEE conference on computer vision and pattern recognition*, 2016, pp. 3364–3372.

[24] J. Shotton, B. Glocker, C. Zach, S. Izadi, A. Criminisi, and A. Fitzgibbon, "Scene coordinate regression forests for camera re-localization in rgb-d images," in *Proceedings of the IEEE Conference on Computer Vision and Pattern Recognition*, 2013, pp. 2930–2937.

[25] T. Hodař, J. Matas, and Š. Obdržálek, "On evaluation of 6d object pose estimation," in *European Conference on Computer Vision*. Springer, 2016, pp. 606–619.

[26] Y. Xiang, T. Schmidt, V. Narayanan, and D. Fox, "Posecnn: A convolutional neural network for 6d object pose estimation in cluttered scenes," *arXiv preprint arXiv:1711.00199*, 2017.

[27] A. Geiger, P. Lenz, and R. Urtasun, "Are we ready for autonomous driving? the kitti vision benchmark suite," in *2012 IEEE Conference on Computer Vision and Pattern Recognition*. IEEE, 2012, pp. 3354–3361.

[28] H. Wang, S. Sridhar, J. Huang, J. Valentin, S. Song, and L. J. Guibas, "Normalized object coordinate space for category-level 6d object pose and size estimation," in *Proceedings of the IEEE/CVF Conference on Computer Vision and Pattern Recognition*, 2019, pp. 2642–2651.

[29] A. Ahmadyan, L. Zhang, J. Wei, A. Ablavatski, and M. Grundmann, "Objectron: A large scale dataset of object-centric videos in the wild with pose annotations," *arXiv preprint arXiv:2012.09988*, 2020.

[30] T. Hodan, P. Haluza, Š. Obdržálek, J. Matas, M. Lourakis, and X. Zabulis, "T-less: An rgb-d dataset for 6d pose estimation of texture-less objects," in *2017 IEEE Winter Conference on Applications of Computer Vision (WACV)*. IEEE, 2017, pp. 880–888.

[31] R. Kaskman, S. Zakharov, I. Shugurov, and S. Ilic, "Home-breweddb: Rgb-d dataset for 6d pose estimation of 3d objects," in *Proceedings of the IEEE/CVF International Conference on Computer Vision Workshops*, 2019, pp. 0–0.

[32] X. Huang, X. Cheng, Q. Geng, B. Cao, D. Zhou, P. Wang, Y. Lin, and R. Yang, "The apolloscape dataset for autonomous driving," in *Proceedings of the IEEE Conference on Computer Vision and Pattern Recognition Workshops*, 2018, pp. 954–960.

[33] B. Calli, A. Singh, A. Walsman, S. Srinivasa, P. Abbeel, and A. M. Dollar, "The ycb object and model set: Towards common benchmarks for manipulation research," in *2015 international conference on advanced robotics (ICAR)*. IEEE, 2015, pp. 510–517.

[34] A. X. Chang, T. Funkhouser, L. Guibas, P. Hanrahan, Q. Huang, Z. Li, S. Savarese, M. Savva, S. Song, H. Su *et al.*, "Shapenet: An information-rich 3d model repository," *arXiv preprint arXiv:1512.03012*, 2015.

[35] W. Kehl, F. Manhardt, F. Tombari, S. Ilic, and N. Navab, "Ssd-6d: Making rgb-based 3d detection and 6d pose estimation great again," in *Proceedings of the IEEE international conference on computer vision*, 2017, pp. 1521–1529.

[36] W. Liu, D. Anguelov, D. Erhan, C. Szegedy, S. Reed, C.-Y. Fu, and A. C. Berg, "Ssd: Single shot multibox detector," in *European conference on computer vision*. Springer, 2016, pp. 21–37.

[37] A. Trabelsi, M. Chaabane, N. Blanchard, and R. Beveridge, "A pose proposal and refinement network for better 6d object pose estimation," in *Proceedings of the IEEE/CVF Winter Conference on Applications of Computer Vision*, 2021, pp. 2382–2391.

[38] Y. Bukschat and M. Vetter, "Efficientpose—an efficient, accurate and scalable end-to-end 6d multi object pose estimation approach," *arXiv preprint arXiv:2011.04307*, 2020.

[39] M. Tan, R. Pang, and Q. V. Le, "Efficientdet: Scalable and efficient object detection," in *Proceedings of the IEEE/CVF conference on computer vision and pattern recognition*, 2020, pp. 10781–10790.

[40] Y. Hu, P. Fua, W. Wang, and M. Salzmann, "Single-stage 6d object pose estimation," in *Proceedings of the IEEE/CVF conference on computer vision and pattern recognition*, 2020, pp. 2930–2939.

[41] B. Chen, A. Parra, J. Cao, N. Li, and T.-J. Chin, "End-to-end learnable geometric vision by backpropagating pnp optimization," in *Proceedings of the IEEE/CVF Conference on Computer Vision and Pattern Recognition*, 2020, pp. 8100–8109.

[42] G. Wang, F. Manhardt, F. Tombari, and X. Ji, "Gdr-net: Geometry-guided direct regression network for monocular 6d object pose estimation," *arXiv preprint arXiv:2102.12145*, 2021.

[43] V. Lepetit, F. Moreno-Noguer, and P. Fua, "Epnp: An accurate o (n) solution to the pnp problem," *International journal of computer vision*, vol. 81, no. 2, p. 155, 2009.

[44] K. He, X. Zhang, S. Ren, and J. Sun, "Deep residual learning for image recognition," in *Proceedings of the IEEE conference on computer vision and pattern recognition*, 2016, pp. 770–778.

[45] M. Rad and V. Lepetit, "Bb8: A scalable, accurate, robust to partial occlusion method for predicting the 3d poses of challenging objects without using depth," in *Proceedings of the IEEE International Conference on Computer Vision*, 2017, pp. 3828–3836.

[46] B. Tekin, S. N. Sinha, and P. Fua, "Real-time seamless single shot 6d object pose prediction," in *Proceedings of the IEEE Conference on Computer Vision and Pattern Recognition*, 2018, pp. 292–301.

[47] J. Redmon, S. Divvala, R. Girshick, and A. Farhadi, "You only look once: Unified, real-time object detection," in *Proceedings of the IEEE conference on computer vision and pattern recognition*, 2016, pp. 779–788.

[48] G. Pavlakos, X. Zhou, A. Chan, K. G. Derpanis, and K. Daniilidis, "6-dof object pose from semantic keypoints," in *2017 IEEE international conference on robotics and automation (ICRA)*. IEEE, 2017, pp. 2011–2018.

[49] Z. Zhao, G. Peng, H. Wang, H.-S. Fang, C. Li, and C. Lu, "Estimating 6d pose from localizing designated surface keypoints," *arXiv preprint arXiv:1812.01387*, 2018.

[50] M. Oberweger, M. Rad, and V. Lepetit, "Making deep heatmaps robust to partial occlusions for 3d object pose estimation," in *Proceedings of the European Conference on Computer Vision (ECCV)*, 2018, pp. 119–134.

[51] Y. Hu, J. Hugonot, P. Fua, and M. Salzmann, "Segmentation-driven 6d object pose estimation," in *Proceedings of the IEEE/CVF Conference on Computer Vision and Pattern Recognition*, 2019, pp. 3385–3394.

[52] S. Peng, Y. Liu, Q. Huang, X. Zhou, and H. Bao, "Pvnet: Pixelwise voting network for 6dof pose estimation," in *Proceedings of*

the IEEE/CVF Conference on Computer Vision and Pattern Recognition, 2019, pp. 4561–4570.

[53] X. Yu, Z. Zhuang, P. Koniusz, and H. Li, “6dof object pose estimation via differentiable proxy voting loss,” *arXiv preprint arXiv:2002.03923*, 2020.

[54] C. Song, J. Song, and Q. Huang, “Hybridpose: 6d object pose estimation under hybrid representations,” in *Proceedings of the IEEE/CVF conference on computer vision and pattern recognition*, 2020, pp. 431–440.

[55] A. Krull, F. Michel, E. Brachmann, S. Gumhold, S. Ihrke, and C. Rother, “6-dof model based tracking via object coordinate regression,” in *Asian Conference on Computer Vision*. Springer, 2014, pp. 384–399.

[56] A. Nigam, A. Penate-Sanchez, and L. Agapito, “Detect globally, label locally: Learning accurate 6-dof object pose estimation by joint segmentation and coordinate regression,” *IEEE Robotics and Automation Letters*, vol. 3, no. 4, pp. 3960–3967, 2018.

[57] Z. Li, G. Wang, and X. Ji, “Cdpn: Coordinates-based disentangled pose network for real-time rgb-based 6-dof object pose estimation,” in *Proceedings of the IEEE/CVF International Conference on Computer Vision*, 2019, pp. 7678–7687.

[58] K. Park, T. Patten, and M. Vincze, “Pix2pose: Pixel-wise coordinate regression of objects for 6d pose estimation,” in *Proceedings of the IEEE/CVF International Conference on Computer Vision*, 2019, pp. 7668–7677.

[59] S. Zakharov, I. Shugurov, and S. Ilic, “Dpod: 6d pose object detector and refiner,” in *Proceedings of the IEEE/CVF International Conference on Computer Vision*, 2019, pp. 1941–1950.

[60] T. Hodan, D. Barath, and J. Matas, “Epos: estimating 6d pose of objects with symmetries,” in *Proceedings of the IEEE/CVF conference on computer vision and pattern recognition*, 2020, pp. 11703–11712.

[61] Y. Li, G. Wang, X. Ji, Y. Xiang, and D. Fox, “Deepim: Deep iterative matching for 6d pose estimation,” in *Proceedings of the European Conference on Computer Vision (ECCV)*, 2018, pp. 683–698.

[62] F. Manhardt, W. Kehl, N. Navab, and F. Tombari, “Deep model-based 6d pose refinement in rgb,” in *Proceedings of the European Conference on Computer Vision (ECCV)*, 2018, pp. 800–815.

[63] L. Yen-Chen, P. Florence, J. T. Barron, A. Rodriguez, P. Isola, and T.-Y. Lin, “Inerf: Inverting neural radiance fields for pose estimation,” *arXiv preprint arXiv:2012.05877*, 2020.

[64] M. Sundermeyer, Z.-C. Marton, M. Durner, M. Brucker, and R. Triebel, “Implicit 3d orientation learning for 6d object detection from rgb images,” in *Proceedings of the European Conference on Computer Vision (ECCV)*, 2018, pp. 699–715.

[65] G. Wang, F. Manhardt, J. Shao, X. Ji, N. Navab, and F. Tombari, “Self6d: Self-supervised monocular 6d object pose estimation,” in *European Conference on Computer Vision*. Springer, 2020, pp. 108–125.

[66] J. Sock, G. Garcia-Hernando, A. Armagan, and T.-K. Kim, “Introducing pose consistency and warp-alignment for self-supervised 6d object pose estimation in color images,” in *2020 International Conference on 3D Vision (3DV)*. IEEE, 2020, pp. 291–300.

[67] Z. Li, Y. Hu, M. Salzmann, and X. Ji, “Robust rgb-based 6-dof pose estimation without real pose annotations,” *arXiv preprint arXiv:2008.08391*, 2020.

[68] Z. Yang, X. Yu, and Y. Yang, “Dsc-posenet: Learning 6dof object pose estimation via dual-scale consistency,” *arXiv preprint arXiv:2104.03658*, 2021.

[69] J. Tobin, R. Fong, A. Ray, J. Schneider, W. Zaremba, and P. Abbeel, “Domain randomization for transferring deep neural networks from simulation to the real world,” in *2017 IEEE/RSJ international conference on intelligent robots and systems (IROS)*. IEEE, 2017, pp. 23–30.

[70] Y. Movshovitz-Attias, T. Kanade, and Y. Sheikh, “How useful is photo-realistic rendering for visual learning?” in *European Conference on Computer Vision*. Springer, 2016, pp. 202–217.

[71] B. Wen, C. Mitash, B. Ren, and K. E. Bekris, “se (3)-tracknet: Data-driven 6d pose tracking by calibrating image residuals in synthetic domains,” *arXiv preprint arXiv:2007.13866*, 2020.

[72] X. Deng, Y. Xiang, A. Mousavian, C. Eppner, T. Bretl, and D. Fox, “Self-supervised 6d object pose estimation for robot manipulation,” in *2020 IEEE International Conference on Robotics and Automation (ICRA)*. IEEE, 2020, pp. 3665–3671.

[73] W. Chen, J. Gao, H. Ling, E. J. Smith, J. Lehtinen, A. Jacobson, and S. Fidler, “Learning to predict 3d objects with an interpolation-based differentiable renderer,” *arXiv preprint arXiv:1908.01210*, 2019.

[74] C. Wang, D. Xu, Y. Zhu, R. Martín-Martín, C. Lu, L. Fei-Fei, and S. Savarese, “Densefusion: 6d object pose estimation by iterative dense fusion,” in *Proceedings of the IEEE/CVF Conference on Computer Vision and Pattern Recognition*, 2019, pp. 3343–3352.

[75] K. Wada, E. Sucar, S. James, D. Lenton, and A. J. Davison, “Morefusion: multi-object reasoning for 6d pose estimation from volumetric fusion,” in *Proceedings of the IEEE/CVF conference on computer vision and pattern recognition*, 2020, pp. 14540–14549.

[76] Y. He, W. Sun, H. Huang, J. Liu, H. Fan, and J. Sun, “Pvn3d: A deep point-wise 3d keypoints voting network for 6dof pose estimation,” in *Proceedings of the IEEE/CVF conference on computer vision and pattern recognition*, 2020, pp. 11632–11641.

[77] G. Gao, M. Lauri, Y. Wang, X. Hu, J. Zhang, and S. Frintrop, “6d object pose regression via supervised learning on point clouds,” in *2020 IEEE International Conference on Robotics and Automation (ICRA)*. IEEE, 2020, pp. 3643–3649.

[78] W. Chen, X. Jia, H. J. Chang, J. Duan, and A. Leonardis, “G2lnet: global to local network for real-time 6d pose estimation with embedding vector features,” in *Proceedings of the IEEE/CVF conference on computer vision and pattern recognition*, 2020, pp. 4233–4242.

[79] G. Gao, M. Lauri, X. Hu, J. Zhang, and S. Frintrop, “Cloudaae: Learning 6d object pose regression with on-line data synthesis on point clouds,” *arXiv preprint arXiv:2103.01977*, 2021.

[80] Y. Wu, M. Zand, A. Etemad, and M. Greenspan, “Vote from the center: 6 dof pose estimation in rgb-d images by radial keypoint voting,” *arXiv preprint arXiv:2104.02527*, 2021.

[81] Y. He, H. Huang, H. Fan, Q. Chen, and J. Sun, “Ffb6d: A full flow bidirectional fusion network for 6d pose estimation,” *arXiv preprint arXiv:2103.02242*, 2021.

[82] D. P. Huttenlocher, G. A. Klanderman, and W. J. Rucklidge, “Comparing images using the hausdorff distance,” *IEEE Transactions on pattern analysis and machine intelligence*, vol. 15, no. 9, pp. 850–863, 1993.

[83] C. Steger, “Similarity measures for occlusion, clutter, and illumination invariant object recognition,” in *Joint Pattern Recognition Symposium*. Springer, 2001, pp. 148–154.

[84] S. Hinterstoisser, C. Cagniart, S. Ilic, P. Sturm, N. Navab, P. Fua, and V. Lepetit, “Gradient response maps for real-time detection of textureless objects,” *IEEE transactions on pattern analysis and machine intelligence*, vol. 34, no. 5, pp. 876–888, 2011.

[85] S. Hinterstoisser, S. Holzer, C. Cagniart, S. Ilic, K. Konolige, N. Navab, and V. Lepetit, “Multimodal templates for real-time detection of texture-less objects in heavily cluttered scenes,” in *2011 international conference on computer vision*. IEEE, 2011, pp. 858–865.

[86] W. Kehl, F. Milletari, F. Tombari, S. Ilic, and N. Navab, “Deep learning of local rgb-d patches for 3d object detection and 6d pose estimation,” in *European conference on computer vision*. Springer, 2016, pp. 205–220.

[87] J. Masci, U. Meier, D. Cireşan, and J. Schmidhuber, “Stacked convolutional auto-encoders for hierarchical feature extraction,” in *International conference on artificial neural networks*. Springer, 2011, pp. 52–59.

[88] K. Park, T. Patten, J. Prankl, and M. Vincze, “Multi-task template matching for object detection, segmentation and pose estimation using depth images,” in *2019 International Conference on Robotics and Automation (ICRA)*. IEEE, 2019, pp. 7207–7213.

[89] P. Wohlhart and V. Lepetit, “Learning descriptors for object recognition and 3d pose estimation,” in *Proceedings of the IEEE conference on computer vision and pattern recognition*, 2015, pp. 3109–3118.

[90] V. Balntas, A. Doumanoglou, C. Sahin, J. Sock, R. Kouskouridas, and T.-K. Kim, “Pose guided rgbd feature learning for 3d object pose estimation,” in *Proceedings of the IEEE international conference on computer vision*, 2017, pp. 3856–3864.

[91] S. Zakharov, W. Kehl, B. Planche, A. Hutter, and S. Ilic, “3d object instance recognition and pose estimation using triplet loss with dynamic margin,” in *2017 IEEE/RSJ International Conference on Intelligent Robots and Systems (IROS)*. IEEE, 2017, pp. 552–559.

[92] W. Chen, J. Duan, H. Basevi, H. J. Chang, and A. Leonardis, “Pointposenet: Point pose network for robust 6d object pose estimation,” in *Proceedings of the IEEE/CVF Winter Conference on Applications of Computer Vision*, 2020, pp. 2824–2833.

[93] D. G. Lowe, "Distinctive image features from scale-invariant keypoints," *International journal of computer vision*, vol. 60, no. 2, pp. 91–110, 2004.

[94] A. Krull, E. Brachmann, F. Michel, M. Y. Yang, S. Gumhold, and C. Rother, "Learning analysis-by-synthesis for 6d pose estimation in rgbd images," in *Proceedings of the IEEE international conference on computer vision*, 2015, pp. 954–962.

[95] O. H. Jafari, S. K. Mustikovela, K. Pertsch, E. Brachmann, and C. Rother, "ipose: instance-aware 6d pose estimation of partly occluded objects," in *Asian Conference on Computer Vision*. Springer, 2018, pp. 477–492.

[96] X. Chen, Y. Chen, B. You, J. Xie, and H. Najjaran, "Detecting 6d poses of target objects from cluttered scenes by learning to align the point cloud patches with the cad models," *IEEE Access*, vol. 8, pp. 210 640–210 650, 2020.

[97] X. Chen, K. Kundu, Z. Zhang, H. Ma, S. Fidler, and R. Urtasun, "Monocular 3d object detection for autonomous driving," in *Proceedings of the IEEE Conference on Computer Vision and Pattern Recognition*, 2016, pp. 2147–2156.

[98] A. Mousavian, D. Anguelov, J. Flynn, and J. Kosecka, "3d bounding box estimation using deep learning and geometry," in *Proceedings of the IEEE Conference on Computer Vision and Pattern Recognition*, 2017, pp. 7074–7082.

[99] B. Li, W. Ouyang, L. Sheng, X. Zeng, and X. Wang, "Gs3d: An efficient 3d object detection framework for autonomous driving," in *Proceedings of the IEEE/CVF Conference on Computer Vision and Pattern Recognition*, 2019, pp. 1019–1028.

[100] L. Liu, J. Lu, C. Xu, Q. Tian, and J. Zhou, "Deep fitting degree scoring network for monocular 3d object detection," in *Proceedings of the IEEE/CVF Conference on Computer Vision and Pattern Recognition*, 2019, pp. 1057–1066.

[101] F. Manhardt, W. Kehl, and A. Gaidon, "Roi-10d: Monocular lifting of 2d detection to 6d pose and metric shape," in *Proceedings of the IEEE/CVF Conference on Computer Vision and Pattern Recognition*, 2019, pp. 2069–2078.

[102] Z. Qin, J. Wang, and Y. Lu, "Monogrnet: A geometric reasoning network for monocular 3d object localization," in *Proceedings of the AAAI Conference on Artificial Intelligence*, vol. 33, no. 01, 2019, pp. 8851–8858.

[103] A. Simonelli, S. R. Bulo, L. Porzi, M. López-Antequera, and P. Kotschieder, "Disentangling monocular 3d object detection," in *Proceedings of the IEEE/CVF International Conference on Computer Vision*, 2019, pp. 1991–1999.

[104] G. Brazil and X. Liu, "M3d-rpn: Monocular 3d region proposal network for object detection," in *Proceedings of the IEEE/CVF International Conference on Computer Vision*, 2019, pp. 9287–9296.

[105] Z. Liu, Z. Wu, and R. Tóth, "Smoke: single-stage monocular 3d object detection via keypoint estimation," in *Proceedings of the IEEE/CVF Conference on Computer Vision and Pattern Recognition Workshops*, 2020, pp. 996–997.

[106] E. Jørgensen, C. Zach, and F. Kahl, "Monocular 3d object detection and box fitting trained end-to-end using intersection-over-union loss," *arXiv preprint arXiv:1906.08070*, 2019.

[107] Y. Wang, W.-L. Chao, D. Garg, B. Hariharan, M. Campbell, and K. Q. Weinberger, "Pseudo-lidar from visual depth estimation: Bridging the gap in 3d object detection for autonomous driving," in *Proceedings of the IEEE/CVF Conference on Computer Vision and Pattern Recognition*, 2019, pp. 8445–8453.

[108] X. Weng and K. Kitani, "Monocular 3d object detection with pseudo-lidar point cloud," in *Proceedings of the IEEE/CVF International Conference on Computer Vision Workshops*, 2019, pp. 0–0.

[109] X. Ma, Z. Wang, H. Li, P. Zhang, W. Ouyang, and X. Fan, "Accurate monocular 3d object detection via color-embedded 3d reconstruction for autonomous driving," in *Proceedings of the IEEE/CVF International Conference on Computer Vision*, 2019, pp. 6851–6860.

[110] J. Feng, E. Ding, and S. Wen, "Monocular 3d object detection via feature domain adaptation."

[111] X. Ma, S. Liu, Z. Xia, H. Zhang, X. Zeng, and W. Ouyang, "Rethinking pseudo-lidar representation," in *European Conference on Computer Vision*. Springer, 2020, pp. 311–327.

[112] M. Ding, Y. Huo, H. Yi, Z. Wang, J. Shi, Z. Lu, and P. Luo, "Learning depth-guided convolutions for monocular 3d object detection," in *Proceedings of the IEEE/CVF Conference on Computer Vision and Pattern Recognition Workshops*, 2020, pp. 1000–1001.

[113] T. Gao, H. Pan, and H. Gao, "Monocular 3d object detection with sequential feature association and depth hint augmentation," *arXiv preprint arXiv:2011.14589*, 2020.

[114] X. Zhou, Y. Peng, C. Long, F. Ren, and C. Shi, "Monet3d: Towards accurate monocular 3d object localization in real time," in *International Conference on Machine Learning*. PMLR, 2020, pp. 11 503–11 512.

[115] P. Li, H. Zhao, P. Liu, and F. Cao, "Rtm3d: Real-time monocular 3d detection from object keypoints for autonomous driving," *arXiv preprint arXiv:2001.03343*, vol. 2, 2020.

[116] X. Shi, Z. Chen, and T.-K. Kim, "Distance-normalized unified representation for monocular 3d object detection," in *European Conference on Computer Vision*. Springer, 2020, pp. 91–107.

[117] L. Liu, C. Wu, J. Lu, L. Xie, J. Zhou, and Q. Tian, "Reinforced axial refinement network for monocular 3d object detection," in *European Conference on Computer Vision*. Springer, 2020, pp. 540–556.

[118] G. Brazil, G. Pons-Moll, X. Liu, and B. Schiele, "Kinematic 3d object detection in monocular video," in *European Conference on Computer Vision*. Springer, 2020, pp. 135–152.

[119] P. Li and Z. Huaici, "Monocular 3d detection with geometric constraint embedding and semi-supervised training," *IEEE Robotics and Automation Letters*, 2021.

[120] Y. Liu, Y. Yixuan, and M. Liu, "Ground-aware monocular 3d object detection for autonomous driving," *IEEE Robotics and Automation Letters*, vol. 6, no. 2, pp. 919–926, 2021.

[121] C. Reading, A. Harakeh, J. Chae, and S. L. Waslander, "Categorical depth distribution network for monocular 3d object detection," *arXiv preprint arXiv:2103.01100*, 2021.

[122] L. Peng, F. Liu, S. Yan, X. He, and D. Cai, "Ocm3d: Object-centric monocular 3d object detection," *arXiv preprint arXiv:2104.06041*, 2021.

[123] L. Peng, F. Liu, Z. Yu, S. Yan, D. Deng, and D. Cai, "Lidar point cloud guided monocular 3d object detection," *arXiv preprint arXiv:2104.09035*, 2021.

[124] Y. Guo, H. Wang, Q. Hu, H. Liu, L. Liu, and M. Bennamoun, "Deep learning for 3d point clouds: A survey," *IEEE transactions on pattern analysis and machine intelligence*, 2020.

[125] D. Fernandes, A. Silva, R. Névoa, C. Simões, D. Gonzalez, M. Guevara, P. Novais, J. Monteiro, and P. Melo-Pinto, "Point-cloud based 3d object detection and classification methods for self-driving applications: A survey and taxonomy," *Information Fusion*, vol. 68, pp. 161–191, 2021.

[126] E. Arnold, O. Y. Al-Jarrah, M. Dianati, S. Fallah, D. Oxtoby, and A. Mouzakitis, "A survey on 3d object detection methods for autonomous driving applications," *IEEE Transactions on Intelligent Transportation Systems*, vol. 20, no. 10, pp. 3782–3795, 2019.

[127] S. Ren, K. He, R. Girshick, and J. Sun, "Faster r-cnn: towards real-time object detection with region proposal networks," *IEEE transactions on pattern analysis and machine intelligence*, vol. 39, no. 6, pp. 1137–1149, 2016.

[128] M. Siam, S. Valipour, M. Jagersand, and N. Ray, "Convolutional gated recurrent networks for video segmentation," in *2017 IEEE international conference on image processing (ICIP)*. IEEE, 2017, pp. 3090–3094.

[129] Y. You, Y. Wang, W.-L. Chao, D. Garg, G. Pleiss, B. Hariharan, M. Campbell, and K. Q. Weinberger, "Pseudo-lidar++: Accurate depth for 3d object detection in autonomous driving," *arXiv preprint arXiv:1906.06310*, 2019.

[130] R. Qian, D. Garg, Y. Wang, Y. You, S. Belongie, B. Hariharan, M. Campbell, K. Q. Weinberger, and W.-L. Chao, "End-to-end pseudo-lidar for image-based 3d object detection," in *Proceedings of the IEEE/CVF Conference on Computer Vision and Pattern Recognition*, 2020, pp. 5881–5890.

[131] A. Simonelli, S. R. Bulò, L. Porzi, P. Kotschieder, and E. Ricci, "Demystifying pseudo-lidar for monocular 3d object detection," *arXiv preprint arXiv:2012.05796*, 2020.

[132] M. Tian, M. H. Ang, and G. H. Lee, "Shape prior deformation for categorical 6d object pose and size estimation," in *European Conference on Computer Vision*. Springer, 2020, pp. 530–546.

[133] D. Chen, J. Li, Z. Wang, and K. Xu, "Learning canonical shape space for category-level 6d object pose and size estimation," in *Proceedings of the IEEE/CVF conference on computer vision and pattern recognition*, 2020, pp. 11 973–11 982.

[134] F. Manhardt, G. Wang, B. Busam, M. Nickel, S. Meier, L. Minicullo, X. Ji, and N. Navab, "Cps++: Improving class-level 6d pose and shape estimation from monocular images with self-supervised learning," *arXiv e-prints*, pp. arXiv–2003, 2020.

[135] J. Lin, Z. Wei, Z. Li, S. Xu, K. Jia, and Y. Li, "Dualposenet: Category-level 6d object pose and size estimation using dual pose network with refined learning of pose consistency," *arXiv preprint arXiv:2103.06526*, 2021.

[136] W. Chen, X. Jia, H. J. Chang, J. Duan, L. Shen, and A. Leonardis, "Fs-net: Fast shape-based network for category-level 6d object pose estimation with decoupled rotation mechanism," *arXiv preprint arXiv:2103.07054*, 2021.

[137] C. Sahin, G. Garcia-Hernando, J. Sock, and T.-K. Kim, "Instance- and category-level 6d object pose estimation," in *RGB-D Image Analysis and Processing*. Springer, 2019, pp. 243–265.

[138] C. Sahin and T.-K. Kim, "Category-level 6d object pose recovery in depth images," in *Proceedings of the European Conference on Computer Vision (ECCV) Workshops*, 2018, pp. 0–0.

[139] K. He, G. Gkioxari, P. Dollár, and R. Girshick, "Mask r-cnn," in *Proceedings of the IEEE international conference on computer vision*, 2017, pp. 2961–2969.

[140] S. Umeyama, "Least-squares estimation of transformation parameters between two point patterns," *IEEE Computer Architecture Letters*, vol. 13, no. 04, pp. 376–380, 1991.

[141] C. R. Qi, H. Su, K. Mo, and L. J. Guibas, "Pointnet: Deep learning on point sets for 3d classification and segmentation," in *Proceedings of the IEEE conference on computer vision and pattern recognition*, 2017, pp. 652–660.

[142] C. Esteves, C. Allen-Blanchette, A. Makadia, and K. Daniilidis, "Learning so (3) equivariant representations with spherical cnns," in *Proceedings of the European Conference on Computer Vision (ECCV)*, 2018, pp. 52–68.

[143] T. Hou, A. Ahmadyan, L. Zhang, J. Wei, and M. Grundmann, "Mobilepose: Real-time pose estimation for unseen objects with weak shape supervision," *arXiv preprint arXiv:2003.03522*, 2020.

[144] M. Sandler, A. Howard, M. Zhu, A. Zhmoginov, and L.-C. Chen, "Mobilenetv2: Inverted residuals and linear bottlenecks," in *Proceedings of the IEEE conference on computer vision and pattern recognition*, 2018, pp. 4510–4520.

[145] M. Tan and Q. Le, "Efficientnet: Rethinking model scaling for convolutional neural networks," in *International Conference on Machine Learning*. PMLR, 2019, pp. 6105–6114.

[146] X. Chen, Z. Dong, J. Song, A. Geiger, and O. Hilliges, "Category level object pose estimation via neural analysis-by-synthesis," in *European Conference on Computer Vision*. Springer, 2020, pp. 139–156.

[147] X. Li, H. Wang, L. Yi, L. J. Guibas, A. L. Abbott, and S. Song, "Category-level articulated object pose estimation," in *Proceedings of the IEEE/CVF Conference on Computer Vision and Pattern Recognition*, 2020, pp. 3706–3715.

[148] M. Garon and J.-F. Lalonde, "Deep 6-dof tracking," *IEEE transactions on visualization and computer graphics*, vol. 23, no. 11, pp. 2410–2418, 2017.

[149] I. Marougas, P. Koutras, N. Kardaris, G. Retsinas, G. Chalatzaki, and P. Maragos, "How to track your dragon: A multi-attentional framework for real-time rgb-d 6-dof object pose tracking," in *European Conference on Computer Vision*. Springer, 2020, pp. 682–699.

[150] A. Dosovitskiy, P. Fischer, E. Ilg, P. Hausser, C. Hazirbas, V. Golkov, P. Van Der Smagt, D. Cremers, and T. Brox, "Flownet: Learning optical flow with convolutional networks," in *Proceedings of the IEEE international conference on computer vision*, 2015, pp. 2758–2766.

[151] B. Busam, H. J. Jung, and N. Navab, "I like to move it: 6d pose estimation as an action decision process," *arXiv preprint arXiv:2009.12678*, 2020.

[152] X. Deng, A. Mousavian, Y. Xiang, F. Xia, T. Bretl, and D. Fox, "Poserbpf: A rao-blackwellized particle filter for 6d object pose tracking," *arXiv preprint arXiv:1905.09304*, 2019.

[153] M. Majcher and B. Kwolek, "3d model-based 6d object pose tracking on rgb images using particle filtering and heuristic optimization," in *VISIGRAPP (5: VISAPP)*, 2020, pp. 690–697.

[154] L. Zhong, Y. Zhang, H. Zhao, A. Chang, W. Xiang, S. Zhang, and L. Zhang, "Seeing through the occluders: Robust monocular 6-dof object pose tracking via model-guided video object segmentation," *IEEE Robotics and Automation Letters*, vol. 5, no. 4, pp. 5159–5166, 2020.

[155] H.-N. Hu, Q.-Z. Cai, D. Wang, J. Lin, M. Sun, P. Krahenbuhl, T. Darrell, and F. Yu, "Joint monocular 3d vehicle detection and tracking," in *Proceedings of the IEEE/CVF International Conference on Computer Vision*, 2019, pp. 5390–5399.

[156] X. Weng, J. Wang, D. Held, and K. Kitani, "3d multi-object tracking: A baseline and new evaluation metrics," *arXiv preprint arXiv:1907.03961*, 2020.

[157] R. E. Kalman, "A new approach to linear filtering and prediction problems," 1960.

[158] H. W. Kuhn, "The hungarian method for the assignment problem," *Naval research logistics quarterly*, vol. 2, no. 1-2, pp. 83–97, 1955.

[159] X. Weng, Y. Yuan, and K. Kitani, "Joint 3d tracking and forecasting with graph neural network and diversity sampling," *arXiv preprint arXiv:2003.07847*, 2020.

[160] F. Leeb, A. Byravan, and D. Fox, "Motion-nets: 6d tracking of unknown objects in unseen environments using rgb," *arXiv preprint arXiv:1910.13942*, 2019.

[161] S. Hochreiter and J. Schmidhuber, "Long short-term memory," *Neural computation*, vol. 9, no. 8, pp. 1735–1780, 1997.

[162] X. Shi, Z. Chen, H. Wang, D.-Y. Yeung, W.-K. Wong, and W.-c. Woo, "Convolutional lstm network: A machine learning approach for precipitation nowcasting," *arXiv preprint arXiv:1506.04214*, 2015.

[163] X. Zhou, V. Koltun, and P. Krähenbühl, "Tracking objects as points," in *European Conference on Computer Vision*. Springer, 2020, pp. 474–490.

[164] K. Duan, S. Bai, L. Xie, H. Qi, Q. Huang, and Q. Tian, "Centernet: Keypoint triplets for object detection," in *Proceedings of the IEEE/CVF International Conference on Computer Vision*, 2019, pp. 6569–6578.

[165] J. Wei, G. Ye, T. Mullen, M. Grundmann, A. Ahmadyan, and T. Hou, "Instant motion tracking and its applications to augmented reality," *arXiv preprint arXiv:1907.06796*, 2019.

[166] A. Ahmadyan, T. Hou, J. Wei, L. Zhang, A. Ablavatski, and M. Grundmann, "Instant 3d object tracking with applications in augmented reality," *arXiv preprint arXiv:2006.13194*, 2020.

[167] C. Wang, R. Martín-Martín, D. Xu, J. Lv, C. Lu, L. Fei-Fei, S. Savarese, and Y. Zhu, "6-pack: Category-level 6d pose tracker with anchor-based keypoints," in *2020 IEEE International Conference on Robotics and Automation (ICRA)*. IEEE, 2020, pp. 10 059–10 066.

[168] Z. Liu, Y. Lin, Y. Cao, H. Hu, Y. Wei, Z. Zhang, S. Lin, and B. Guo, "Swin transformer: Hierarchical vision transformer using shifted windows," *arXiv preprint arXiv:2103.14030*, 2021.

[169] W. Wang, E. Xie, X. Li, D.-P. Fan, K. Song, D. Liang, T. Lu, P. Luo, and L. Shao, "Pyramid vision transformer: A versatile backbone for dense prediction without convolutions," *arXiv preprint arXiv:2102.12122*, 2021.

[170] G. Chen, W. Choi, X. Yu, T. Han, and M. Chandraker, "Learning efficient object detection models with knowledge distillation," in *Proceedings of the 31st International Conference on Neural Information Processing Systems*, 2017, pp. 742–751.

[171] Y. Kim and A. M. Rush, "Sequence-level knowledge distillation," *arXiv preprint arXiv:1606.07947*, 2016.

[172] C. Zhu, Y. He, and M. Savvides, "Feature selective anchor-free module for single-shot object detection," in *Proceedings of the IEEE/CVF Conference on Computer Vision and Pattern Recognition*, 2019, pp. 840–849.